

University of Louisville

ThinkIR: The University of Louisville's Institutional Repository

Electronic Theses and Dissertations

5-2013

Optimal scheduling for charging electric vehicles with fixed setup costs.

Guangyang Xu
University of Louisville

Follow this and additional works at: <https://ir.library.louisville.edu/etd>

Recommended Citation

Xu, Guangyang, "Optimal scheduling for charging electric vehicles with fixed setup costs." (2013).
Electronic Theses and Dissertations. Paper 1607.
<https://doi.org/10.18297/etd/1607>

This Master's Thesis is brought to you for free and open access by ThinkIR: The University of Louisville's Institutional Repository. It has been accepted for inclusion in Electronic Theses and Dissertations by an authorized administrator of ThinkIR: The University of Louisville's Institutional Repository. This title appears here courtesy of the author, who has retained all other copyrights. For more information, please contact thinkir@louisville.edu.

**OPTIMAL SCHEDULING FOR CHARGING ELECTRIC
VEHICLES WITH FIXED SETUP COSTS**

By

Guangyang Xu
B.S., China University of Mining and Technology, 2004

A Thesis
Submitted to the Faculty of the
J.B. Speed School of Engineering of the University of Louisville
in Partial Fulfillment of the Requirements
for the Degree of

Master of Science

Department of Industrial Engineering
University of Louisville
Louisville, Kentucky

May 2013

OPTIMAL SCHEDULING FOR CHARGING ELECTRIC VEHICLES WITH FIXED
SETUP COSTS

Submitted by:

Guangyang Xu

A Thesis Approved on

4/22/2013

(Date)

by the following Reading and Examination Committee:

Dr. Lihui Bai, Thesis Director

Dr. Gerald W. Evans

Dr. Michael L. McIntyre

ACKNOWLEDGEMENTS

I would like to express my deepest gratitude to my thesis advisor, Dr. Lihui Bai, for her never ending support and motivation. Her guidance along the way was really valuable and her patience and encouragements never failed to make me feel confident again in the research that I am doing. My sincere thanks go to Dr. Gerald W. Evans and Dr. Michael L. McIntyre for reviewing and providing some comments to improve this thesis. My appreciation also goes to Dr. John Kielkopf for his valuable L^AT_EX template of the thesis.

I would also like to thank Conn Center For Renewable Energy Research for providing me the Leigh Ann Conn Graduate Fellowship and giving me the opportunity to pursue my post-graduate studies here at the University of Louisville.

My greatest appreciation goes to my beloved parents, Baohui Yang and Pingshun Xu for their love and support. Without their trust, I would have never reached this far.

Last but not least, I would like to thank my professors and fellow friends for their support, helpful comments and encouragement. Their help is deeply appreciated.

ABSTRACT

OPTIMAL SCHEDULING FOR CHARGING ELECTRIC VEHICLES WITH FIXED SETUP COSTS

Guangyang Xu

April 22, 2013

The increasing popularity of electric vehicles (EV) will pose great challenge to the nation's existing power grid by adding extra load during evening peak hours. This thesis develops a centralized optimal charging scheduling (OCS) model with a mixed integer nonlinear program to mitigate the negative impact of extra load from EVs on the power grid. The objective of the OCS model is to minimize the energy cost of the entire system and fixed setup costs for day-time charging, which essentially levels the load of the entire power grid throughout a day under the dynamic pricing environment. Furthermore, a rolling horizon heuristic algorithm is proposed as an alternative solution that addresses large scale OCS instances. Finally, when centralized scheduling is impractical, this thesis proposes a decentralized optimal charging heuristic using the concepts of game theory and coordinate search. Numerical results show that the optimal charging scheduling model can significantly lower the total energy cost and the peak-to-average ratio (PAR) for a power system. When compared to uncontrolled charging, the decentralized charging heuristic yields considerable energy savings as well, although not as efficient as the centralized optimal charging solutions.

TABLE OF CONTENTS

	Page
ACKNOWLEDGEMENTS	iii
ABSTRACT	iv
LIST OF TABLES	vii
LIST OF FIGURES	ix
CHAPTER	
1 INTRODUCTION	1
2 LITERATURE REVIEW	5
2.1 Demand Side Management (DSM) in EV Charging	5
2.2 Centralized Optimal Charging Scheduling	7
2.3 Decentralized Charging Scheduling	10
2.4 The Choice of Electricity Cost Function	11
3 MODELS AND ALGORITHMS FOR EV CHARGING	13
3.1 Centralized Optimization Model	13
3.2 A Rolling Horizon Heuristic (RHH) Algorithm	17
3.3 Decentralized Charging Heuristic	20
4 NUMERICAL RESULTS	23
4.1 Data Generation	23
4.2 Results for OCS Models	25
4.2.1 Models Vs. Linear Programming (LP) Relaxation	26
4.2.2 Results for MIP Models vs. Uncontrolled EV Charging .	27
4.2.3 Results for MIP Solutions for Various Fixed Setup Costs	29
4.3 Results for Rolling Horizon Heuristic (RHH)	39
4.4 Results for Decentralized Models	40

5	CONCLUSION AND FUTURE WORK	50
5.1	Conclusions	50
5.2	Future Work	51
	REFERENCES	52
	CURRICULUM VITAE	57

LIST OF TABLES

TABLE		Page
1	Description of variables in Algorithm 1	17
2	Relaxation vs. original OCS model (linear cost, $n = 10$)	27
3	Relaxation vs. original OCS model (linear cost, $n = 100$)	27
4	Results for uncontrolled charging with the linear cost ($n = 10$)	28
5	Results for optimal charging with \$0 fixed cost ($n = 10$)	28
6	Results for optimal charging with \$0.25 fixed cost ($n = 10$)	29
7	Results for optimal charging with \$1 fixed cost ($n = 10$)	29
8	Results for uncontrolled charging with the linear cost ($n = 50$)	30
9	Results for optimal charging with \$0 fixed cost ($n = 50$)	30
10	Results for optimal charging with \$0.25 fixed cost ($n = 50$)	30
11	Results for optimal charging with \$1 fixed cost ($n = 50$)	31
12	Results for uncontrolled charging with the linear cost ($n = 100$)	31
13	Results for optimal charging with \$0 fixed cost ($n = 100$)	31
14	Results for optimal charging with \$0.25 fixed cost ($n = 100$)	32
15	Results for optimal charging with \$1 fixed cost ($n = 100$)	32
16	Results for uncontrolled charging with the linear cost ($n = 200$)	32
17	Results for optimal charging with \$0 fixed cost ($n = 200$)	33
18	Results for optimal charging with \$0.25 fixed cost ($n = 200$)	33
19	Results for optimal charging with \$1 fixed cost ($n = 200$)	33
20	Results of the (OCS) using the linear cost function (Uncontrolled and fc = \$0)	34
21	Results of the (OCS) using the linear cost function (fc = \$0.25 and fc = \$1)	34
22	CPU times for (OCS) charging scenarios	39

23	Results of rolling heuristic and comparison with (OCS) charging scenarios	39
24	Results for decentralized charging with \$0 fixed cost ($n = 10$)	41
25	Results for decentralized charging with \$0.25 fixed cost ($n = 10$)	42
26	Results for decentralized charging with \$1 fixed cost ($n = 10$)	42
27	Results for decentralized charging with \$0 fixed cost ($n = 50$)	42
28	Results for decentralized charging with \$0.25 fixed cost ($n = 50$)	43
29	Results for decentralized charging with \$1 fixed cost ($n = 50$)	43
30	Results for decentralized charging with \$0 fixed cost ($n = 100$)	43
31	Results for decentralized charging with \$0.25 fixed cost ($n = 100$)	44
32	Results for decentralized charging with \$1 fixed cost ($n = 100$)	44
33	Results for decentralized charging with \$0 fixed cost ($n = 200$)	44
34	Results for decentralized charging with \$0.25 fixed cost ($n = 200$)	45
35	Results for decentralized charging with \$1 fixed cost ($n = 200$)	45
36	Comparisons between the (OCS) and (DCS) models under three fixed cost ($n=10$ and $n=50$) scenarios	47
37	Comparisons between the (OCS) and (DCS) models under three fixed cost ($n=100$ and $n=200$) scenarios	48

LIST OF FIGURES

FIGURE		Page
1	The household load profiles in summer months	24
2	Four scenarios of charging profile for user 1 under uncontrolled and OCS model	37
3	Overall load leveling under uncontrolled charging and (OCS) model with different fixed cost ($n=10$)	38
4	Four scenarios of charging profile for user 1 under uncontrolled and DCS model	47
5	Comparison of load leveling under different models ($n=10$)	49

CHAPTER 1

INTRODUCTION

Since the late 1990s, there have been growing concerns on the consumption of fossil fuel due to issues such as energy independence and climate change. Governments around the world are making policy changes to address with these issues. In the U.S., the fuel economy standards on automobiles have been set higher numerous times in the past ten years [1]. In 2004, California became the first state in the U.S. to adopt the Pavley Car Standards [2], followed by 13 other states later. President Obama adopted the standards at the federal level in 2010. These regulations forced the auto industry into a new round of innovation with the effort to make fuel efficient cars. Thus, the market for electric vehicle (EV), which includes battery electric vehicle (BEV) and plug-in hybrid electric vehicle (PHEV), is booming. The number of hybrid or electric vehicles on the road increased from zero in 1991 to two million in 2010 [1]. Consequently, transportation economists have projected the EV market to be strong, with EVs comprising 64 to 86 percent of light vehicle sales in the US by 2030 [3]. On the other hand, as suggested by Rahman and Shrestha [4], large scale deployment of EVs will significantly increase the total electricity power demand (or load) at peak hours, which poses a great challenge for the reliability of the current nation's power grids.

Although some research is done on load leveling and demand side management (see, e.g., [5], [6] and references therein), literature on load leveling via effectively managing charging hours for EVs is rather scant. Rahman and Shrestha [4] study the impact of EV load on the electric utility system. Collins and Mader [7] examine the best timing of EV recharging through two electric utility rate

structures: the fixed and time-of-day rates. In addition, Koyanagi and Uriu [8] develop a model to predict the future demand of electricity by EVs and propose the regional charging time zone method to balance the demand by EVs in various regions. While the above mentioned research focuses on the effectiveness of certain charging/discharging policies under various conditions, it is desirable to have an integrated EV charging scheduling solution. Such a solution should recommend EV users on when and how much to charge their EVs during a day, with the objectives of minimizing the total electricity cost and maximizing the load leveling of the entire power system. The research in this thesis attempts to address this problem.

Particularly, in order to mitigate the negative impact of EV charging on the power grid, load leveling is a desired objective of the optimal charging scheduling solution. Thus this thesis considers the optimal charging scheduling (OCS) problem under the dynamic rate of electricity, i.e., the unit electricity price at any given time is a (monotone) increasing function of the total electricity load at the time. Under the dynamic pricing structure, load leveling can be achieved by minimizing the electricity cost of the entire system. This is because cost minimization will incentivize EV users to shift peak-hour charging to off-peak hours. This further indicates that the OCS model will also reduce the peak-to-average ratio (PAR) for the power systems. Overall, the OCS problem in this thesis is for a central system controller to minimize the total electricity cost incurred by all EV users collectively, while the EV charging demand for each user is satisfied. Such centralized decision models can be practical in many settings. For example, as EV becomes more popular, one envisions that institutions (such as universities and hospitals) own charging stations in their parking facilities, and thus have the authority to arrange charging activities for greater economic efficiency. As another example, in a power distribution system, load aggregators can play the role of central controller and may be interested in coordinating charging activities by (aggregated) users (e.g., all EV users in a pre-defined residential zone).

In essence, the proposed OCS model is a mixed integer nonlinear program that optimally schedules/coordinates EV users charging activities throughout a day.

In addition to minimizing the total electricity costs for all users while meeting their charging demands, considerations are also given to EV users' classification, EV users' various commute schedule and EVs' battery capacity. First, EV users are divided into two groups based on the distance of their daily commute. One group represents short-distance users who travel less than 100 miles per day (round trip) and the other represents medium-distance users who travels between 100 and 150 miles per day (round trip). Note that long-distance users, whose daily commute exceeds 150 miles, are not included in the current study because 90% of U.S. household vehicle trips is less than 100 miles per day according to U.S. Department of Energy [9]. Second, because the EVs currently available on the market have the driving distance of around 100 miles per full charge, the day-time (or at-work) charging becomes necessary for medium-distance users. Therefore it is assumed that day-time charging facilities are available to these users. Third, the OCS model considers EV users' daily commute and does not allow them to charge their EVs during commute. For short and medium distance users, their (one way) commutes per day are one hour and one and half hours, respectively.

One innovative consideration of the OCS model is the fixed setup cost (fc) that is incurred between two non-consecutive charges during the day-time. In other words, every time a user starts a new charge during the day-time period, a setup cost is incurred. Unlike at-home charging during evenings, the day-time 'at-work' charging prefers a strong continuity of charging due to limited resources at public charging stations. The fixed cost in the OCS model can be interpreted as the penalties of non-consecutive charging (PNCC) during the day-time including labor cost required for switching on and off the charger, inconvenience to users, harmful effects on battery's life and the resulting instability of the power grid due to more frequent setups. In addition, it is important to note that the fixed cost is not necessarily the monetary cost to EV users. Instead, it provides a means of increasing the continuity of day-time charging. When including the fixed setup cost, the OCS model becomes computational expensive for a power distribution system with 100 or more EV users. Therefore, the thesis proposes a rolling horizon heuristic

algorithm that provides quality solutions quickly.

Finally, in some situations a decentralized charging scheduling may be more appealing to public, in which EV users (instead of a central controller) determine their own charging schedules. Thus, a decentralized optimal charging heuristic is developed by applying the game theoretical approach (see e.g., [10] and [11]). The goal of the decentralized algorithm is to study interactions among all EV users when each minimizes his/her own total cost (i.e., electricity cost plus the fixed setup cost) and the effect of such ‘selfish’ charging behaviors on the system-wide cost and load profile. Using the same classification of short and medium distance users as in the centralized models, the decentralized scheduling heuristic allows users to learn and adapt day after day. Particularly, on each day a Gauss-Seidel type of coordinate search optimizes each user’s charging schedule given his/her best knowledge on others (charging) activities so far. This decentralized heuristic, although suboptimal compared to centralized models, still improve the system performance considerably with respect to load leveling and cost, when compared to uncoordinated charging.

In summary, the contribution of this thesis is four fold. First, a mathematical model is developed for the centralized charging scheduling problem that explicitly incorporates two groups of EV users, their respective commute schedules, and the “state of charge” dynamics for all EVs. Second, the novel idea of introducing the fixed setup cost helps to reduce the percentage of non-consecutive charge (PNCC). Third, a rolling horizon heuristic algorithm is proposed as an alternative for solving large scale OCS models. Finally, a decentralized/distributed charging heuristic model is developed when centralized controlled charging is not feasible.

The rest of this thesis is organized as follows. Chapter II reviews the literature on optimal charging scheduling, demand side management (DSM) and distributed charging scheduling. Chapter III formulates the centralized model for optimal charging scheduling and proposes a rolling horizon heuristic algorithm for its solution. Chapter IV presents the decentralized charging scheduling heuristic. Chapter V reports the numerical results, and conclusions are presented in Chapter VI.

CHAPTER 2

LITERATURE REVIEW

2.1 Demand Side Management (DSM) in EV Charging

Demand Side Management (DSM) was first introduced by Electric Power Research Institute (EPRI) in the 1980s [12]. It is the modification of consumer demand for energy through various methods such as financial incentives and education. DSM aims to improve final electricity-using systems, reduce consumption, while preserving the same level of service and comfort [13].

In the literature of DSM, many optimization techniques have been used in the energy consumption scheduling solutions. Zhang et al. [14] use mixed-integer linear programming to study the optimal scheduling of smart home's energy consumption. They schedule operation and electricity consumption tasks based on different electricity tariffs, electricity task time window and forecasted renewable energy output in order to minimize a one-day forecasted energy consumption cost. In addition, Zhang et al. [14] conduct a case study of thirty homes in which twelve domestic tasks from thirty homes are scheduled. Compared to the case where the tasks all start at their earliest possible starting time, the electricity consumption peak is decreased from 290kW to 165kW and the electricity consumption pattern becomes flatter.

Quadratic programming is a widely used optimization technique in the DSM literature. Vandael et al. [15] compare several solutions for PHEVs charging scheduling. They benchmark a multi-agent solution against an optimal quadratic programming scheduler solution. The results in [15] show that a quadratic

programming scheduler is able to optimally flatten peak loads while sufficiently charging the PHEV batteries. However, this solution is infeasible in practice because it scales poorly and requires complete information on when and how much PHEVs need to charge beforehand, which is not realistic.

Ramchurn et al. [16] provide a mixed-integer quadratic programming formulation to solve a model of a decentralized demand side management (DDSM). The DDSM model allows agents, by adapting the deferment of their loads based on grid prices, to coordinate in a decentralized manner. They demonstrate that through an emergent coordination of the agents, the peak demand of domestic consumers in the grid can be reduced by up to 17% and carbon emissions by up to 6%. Ramchurn et al. [16] also show that the DDSM mechanism is robust to the increasing electrification of heating in UK homes.

Dynamic programming is another popular technique used in DSM. In order to minimize both dollar and comfort costs associated with utility use and conservation, Kowahl and Kuh [17] propose a softmax algorithm with neighborhood update to implement approximate dynamic programming. The goal is to reduce dependancies on models and forecast while achieving good performance. The simulation results for the softmax algorithm show that the approximate dynamic programming solution approaches the optimal dynamic programming solution.

Clement-Nyns et al. [18] propose a coordinated charging to minimize the power losses and to maximize the main grid load factor. They use both of quadratic and dynamic programming techniques in the study. The computational results of quadratic programming and dynamic programming are shown in the paper, which indicate that dynamic programming does not improve the computational time nor the solution accuracy.

Another stream of research in DSM is the study of various mechanisms to incentivize users to participate and shift their electricity usage to off-peak hours. For example, Mohsenian-Rad et al. [19] consider deployment of energy consumption scheduling (ECS) devices in smart meters for autonomous demand side management within a neighborhood, where several buildings share an energy source. The ECS

devices interact automatically by running a distributed algorithm to find the optimal energy consumption schedule for each subscriber. The incentive in [19] is the dynamic pricing, where the unit electricity price is a linear function of total load. Simulation results in [19] show that: 1) users are motivated to avoid peak hours; 2) the proposed distributed algorithm can reduce the peak-to-average ratio and the total cost in the system.

In a related work, Vytelingum et al. [20] present an agent-based micro-storage management technique that allows all individually-owned storage devices in the system to converge to profitable, efficient behaviour. Specifically, they provide a general framework to analyze the Nash equilibrium of an electricity grid and devise new agent-based storage learning strategies that adapt to market conditions. The results in [20] show that in the UK electricity market, it is possible to achieve savings of up to 13% on average for a consumer on his electricity bill with a storage device of 4 kWh. Moreover, they show that there exists an equilibrium where only 38% of UK households would own storage devices and social welfare would be maximized.

Finally, Fan [21] studies the application of congestion pricing in Internet traffic control for demand response in smart grid. In particular, he proposes to include the ‘willingness to pay’ in the pricing scheme for the DSM for energy consumption scheduling. In [21], user preference is modeled as a ‘willingness to pay’ parameter which can be seen as an indicator of differential quality of service. Both analytical and simulation results demonstrate the dynamics and convergence behavior of the algorithm.

2.2 Centralized Optimal Charging Scheduling

Managing the scheduling of EV charging is a sub-area of DSM, and has been studied rather extensively in the past ten years. In order to mitigate the adverse impact of uncontrolled EV charging on the power grid, coordinated or centralized charging has become more promising with the development of smart grid and its supporting infrastructure. In particular, Clement et al. [22] describe the

uncoordinated charging as that the vehicles are charged immediately when they are plugged in or after a fixed start delay, which can lead to grid problems on a local scale. Therefore, Clement et al. [22] propose a coordinated charging to minimize the power losses and to maximize the main grid load factor. The optimal charging profile of the PHEVs is computed by minimizing the power losses, in which the forecasting of household loads is handled by stochastic programming.

Similarly, Mets et al. [23] investigate the potential benefits of using control mechanisms in optimizing energy consumption stemming from PHEV charging in a residential use case. They present two smart energy control strategies based on quadratic programming for charging PHEVs to minimize the peak load and flatten the overall load profile. Both strategies (local and global iterative) control the duration and rate of charging for each vehicle. Mets et al. [23] show quantitative simulation results over a set of 150 homes, and discuss the strategies in terms of complexity and resulting energy consumption, as well as their infrastructure and communication requirements.

Furthermore, Sundström and Binding [24] study the optimal electric vehicle battery charging behavior in order to minimize charging costs, achieve satisfactory state-of-energy levels, and optimal power balancing. Both linear approximation and quadratic approximation formulations are presented in the research. Sundström and Binding [24] use a non-linear and state-dependent battery model to evaluate the solutions of the two methods. Their results indicate that the linear approximation is sufficient when considering the electric vehicle charging plan optimization.

Another aspect in the optimal charging scheduling for electric vehicles is the electric vehicle's charging pattern. The charging pattern of an electric vehicle depends on the vehicle's usage pattern such as the distance traveled and when the recharging is needed. In the literature, Xu and Pan [25] construct a dynamic stochastic model to study the scheduling problem for battery charging of multiple PHEVs. Moreover, through a dynamic programming formulation, they show that if the non-completion penalty (as a function of the additional time needed to fulfill the unsatisfied charging request) is convex, priority should be given to vehicles that

have less laxity and longer remaining processing times. According to this principle, Xu and Pan [25] propose several improved charging scheduling policies suggested by their heuristic algorithms. These improved policies focus only on improving the social welfare, when compared to the original heuristics.

On the other hand, Rautiainen et al. [26] study the statistical charging load modeling of PHEVs in electricity distribution networks. They investigate the usefulness of the national travel survey data in the modeling. In addition, Rautiainen et al. [26] propose a novel modeling methodology where detailed car use habits are used to produce the statistical distributions of energy consumption from EV charging. The models in [26] can be easily applied to network calculation tools that are commonly used by distribution network operators.

When sources of electricity consumption, other than EV charging, are concerned, numerous literature addresses the general energy consumption scheduling. For example, Mohsenian-Rad and Leon-Garcia [27] propose an optimal and automatic residential energy consumption scheduling framework. Their model considers the trade-off between minimizing the electricity cost and minimizing the waiting time for using each appliance in household under the real-time pricing tariff combined with inclining block rates. The simulation results in [27] show that the combination of the proposed energy consumption scheduling design and the price predictor filter leads to significant reduction not only in users payments but also peak-to-average ratio in load demand for various load scenarios. Therefore, the deployment of the optimal energy consumption scheduling schemes in [27] is beneficial for both end users and utility companies.

Additionally, Samadi et al. [28] model the users' preferences and their energy consumption patterns in form of selected utility functions based on concepts from microeconomics. They also propose a distributed algorithm which finds the optimal energy consumption levels for each subscriber, so that the aggregate utility of all subscribers in the system is maximized in a fair and efficient way. Samadi et al. [28] show that the energy provider can encourage some desirable consumption patterns among the subscribers by the means of real-time pricing. The simulation results

confirm that the proposed distributed algorithm can potentially benefit both subscribers and the energy provider.

2.3 Decentralized Charging Scheduling

Distributed algorithm for coordinated charging, is motivated by individualism in decision making in energy consumption or particularly, EV charging, and has attracted many researchers in the past decades. Compared to centralized optimal charging scheduling, decentralize/distributed scheduling assumes there is no central controller and all individuals decide or optimize their own charging profiles. As a result, the agent-based approach (e.g., [29]) seems to be a good fit to model individuals' consumption behavior. For example, Vytelingum et al. [20] implement the agent-based concept in developing a micro-storage management algorithm for the smart grid. In their model, each agent fixes his or her storage profile based on forecasted market price. Vytelingum et al. [20] prove that the average storage profile from their distributed algorithm converges to the Nash Equilibrium. Consequently, average peak demand induced by the optimal storage profile is reduced, thus eliminating the requirements for more costly and carbon-intensive generation plant.

In addition, Vandael et al. [15] propose a multi-agent solution and compared the qualities of this solution with an optimal reference solution obtained by quadratic programming. They use a decentralized model to level the load at each transformer through two coordination strategies: the energy limiter and power limiter. The former only uses predictions about loads, while the latter doesn't use any forecast data. In [15], the multi-agent solution proves to be scalable and adaptable to incomplete and unpredictable information, while still capable of reducing peak demands with an efficiency up to 95% compared to the quadratic scheduler.

Similarly, Ma et al. [30] develop a strategy to coordinate the charging of autonomous PHEVs using concepts from non-cooperative games. The foundation of their research is a model that assumes PHEVs are cost-minimizing and weakly coupled via a common electricity price. In [30], it is shown that there exists a

unique Nash equilibrium, which is close to a solution that minimizes the electricity generation costs by scheduling PHEV demand to fill the overnight non-PHEV demand valley. This result is accompanied by a decentralized computational algorithm and a proof that the algorithm converges to the Nash equilibrium in the infinite system limit.

Finally, Phan et al. [31] propose a distributed decision-making scheme to model the charging of a collection of EVs, in which each charger individually determines its own charging schedule by iteratively transacting signals with a central authority. The model introduces capacity constraints on the distribution grid, fair rationing of energy supply available under the capacity constraint, and discrete choice of EV charger settings. Phan et al. [31] find that the centralized version of the problem is an mixed integer non-linear programming, which is too hard for standard solvers even with small size instances. Therefore, they present a distributed approximation scheme to solve the large-scale optimization model.

2.4 The Choice of Electricity Cost Function

A crucial element in any DSM study is the choice of the electricity cost/price, which has been studied rather extensively. Most studies on electricity markets incorporate quadratic functions describing the relationship between cost and electric usage. In [32], a piecewise linear approximation is often applied to ease computational burden that would otherwise be experienced by quadratic models. On the other hand, the residential ‘time-of-use’ (TOU) rate has also been actively studied at various U.S. cities through projects funded by the U.S. Department of Energy over the past decades. The first project to implement the residential TOU rate began in 1975 in Vermont and was documented in [33]. The latter provides a detailed analysis of the TOU experiments in residential areas. Aigner [33] concludes that effective pricing mechanism to change consumers’ behavior is among the most important issues to the success of TOU rates. Other studies focusing on the impacts of TOU rates include [7], [34] [35], and [36].

Moreover, Fetz and Filippini [37] have studied the economies of vertical

integration and economies of scale. Specifically, they use different econometric specifications for panel data, including a random effects and a random-coefficients model, to estimate a quadratic multi-stage cost function for a sample of electricity companies. The empirical results in [37] reflect the presence of considerable economies of vertical integration and economies of scale for most companies considered in the analysis. Moreover, the results suggest a variation in economies of vertical integration across companies due to unobserved heterogeneity.

Finally, concerning the production cost, Martínez-Budría et al. [38] have adapted productivity analysis to the case of a cost model. A normalized quadratic cost function is estimated and discrete data has been used in their research. The main theoretical result in [38] is a productivity index that can be decomposed into modified versions of the contribution of technical change and the effect of the variations in the scale of production. The results also show important productivity gains with both technical change and scale effect playing important roles.

The next chapter presents the mathematical models, program formulations and algorithms for the centralized and decentralized charging scheduling.

CHAPTER 3

MODELS AND ALGORITHMS FOR EV CHARGING

3.1 Centralized Optimization Model

The goal of the centralized optimal charging scheduling model is for the power network controller (e.g., aggregator) to schedule a charging profile for each user so that the user’s charging demand is fulfilled while the total cost for all users collectively is minimized. Under the real-time pricing where unit electricity price is a monotone increasing function of the load, minimizing the total cost automatically levels the load for the entire grid throughout the day. Because one objective of the research is to study the adverse effect of EV charging on the power grid, two demand sources for electricity are considered. One is the regular household usage such as heating, lighting, washer and dryer, and the other is the EV charging. Mathematically, let $t \in \{1, 2, \dots, T\}$ denote a time interval in a 24-hour cycle. For example, when $T = 24$, each t represents a one-hour interval and when $T = 48$, each t represents a half-hour interval. Consider a power distribution network with n EV users. Let D_i^t be the regular household demand for user i at time interval t , and d_i be the daily EV charging demand for user i .

Without loss of generality, the proposed OCS model considers BEV users only. If PHEV users need to be included, one simply adjusts the charging demand d_i . Further, BEV users may charge their vehicles from 8am to 5pm, which is termed as “day-time” or “at-work” charging; or from 5pm to 8am the following day, which is termed as “night-time” or “at-home” charging in the thesis. Thus, the OCS model implicitly assumes that commercial charging infrastructure at workplace is

available. In addition, as mentioned previously, two types of EV users are considered based on their travel motion/distance (e.g., [8]). The first type is the short-distance user who travels less than 100 miles (round trip) daily. The second type is the medium-distance user who travels between 100 and 150 miles (round trip) daily. 100 miles distance is chosen as it is a sufficient mileage for more than 90% of all household vehicle trips in the U.S. (see e.g., [7] and [9]). Let \mathcal{M} be the set of medium-distance users. Thus, for any user $i \in \mathcal{M}$ and user $j \notin \mathcal{M}$, $d_i > d_j$.

Let decision variable x_i^t be the amount of charge for user i during time interval t , and y_i^t be the associated binary variable indicating if user i is assigned to charge during interval t . In words, $y_i^t = 1$ when EV user i charges at time interval t , and $y_i^t = 0$ otherwise. Then, the total load v_t at each time interval t is calculated as the sum of regular household load and extra load from EV charging of all users during that particular time interval, i.e., $v_t = \sum_{i=1}^n (D_i^t + x_i^t)$. Let u_i^t be the amount of remaining electricity in battery, i.e., the “state of charge,” for vehicle (user) i at time t . Furthermore, let w_i^t and z_i^t be binary variables so that $w_i^t - z_i^t$ equals 1 if user i starts a new charge at time t , -1 if user i ends a charge at time t and 0 if user i 's charging status is unchanged between time t and $t - 1$. Hence, the total setup cost for user i is calculated as $F \sum_t w_i^t$, where F is the fixed setup cost. Finally, as in [19], the unit electricity price $p_t(v_t) = c_0^t + c^t v_t (c^t \neq 0)$ at time t is a linear function of the total load v_t at time t .

Using the above notation, the OCS model can be formulated as the following

mixed integer program (1)-(11).

$$(OCS) \quad \min f = \sum_{t=1}^T p_t(v_t)v_t + F \sum_{t,i} w_i^t \quad (1)$$

$$\text{s.t. } v_t = \sum_{i=1}^n (D_i^t + x_i^t), \quad \forall t \in \{1, \dots, T\} \quad (2)$$

$$\sum_{t=1}^T x_i^t = d_i, \quad \forall i \in \{1, \dots, n\} \quad (3)$$

$$\sum_{t \in \mathcal{C}_i} y_i^t = 0, \quad \forall i \quad (4)$$

$$x_i^t = \alpha y_i^t, \quad \forall i, t \quad (5)$$

$$u_i^t = u_i^{t-1} + x_i^t - d_i^t, \quad \forall i, t \geq 2 \quad (6)$$

$$u_i^1 = u_i^T + x_i^1 - d_i^1, \quad \forall i \quad (7)$$

$$u_i^t \leq C, \quad \forall i, t \quad (8)$$

$$y_i^t - y_i^{t-1} = w_i^t - z_i^t, \quad \forall i, T_s \leq t \leq T_e \quad (9)$$

$$y_i^{T_s} = w_i^{T_s}, \quad \forall i \quad (10)$$

$$y_i^t \in \{0, 1\}, \quad x_i^t \geq 0, \quad u_i^t \geq 0, \quad w_i^t \geq 0, \quad z_i^t \geq 0, \quad \forall i, t \quad (11)$$

In particular, the objective in equation (1) minimizes the total cost (i.e., the sum of energy and setup costs) for all users in the distribution system. Constraints of the model include equations (2) through (11). Particularly, constraint (2) calculates the total load in each time interval t as the sum of household load and charging demand for all users. Constraint (3) ensures that each EV user's daily charging requirement is fulfilled in a 24-hour cycle. Further, constraint (4) states that no user will charge their EVs while driving for $t \in \mathcal{C}_i$, where \mathcal{C}_i is the set of time intervals for morning and evening commute hours, whose composition depends on the length of interval t . For example, if $T = 48$, then \mathcal{C}_i ranges from 14 to 16 for morning commute hours and from 35 to 37 for evening commute hours. Additionally, constraint (5) assigns a total charge of α kWh to user i ($x_i^t = \alpha$) if the user is determined to charge during time interval t ($y_i^t=1$). Note that α is the energy drawn from the charging station during one unit of time, and its value may

vary among different types of charging stations. Constraints (6) to (8) consider the “state of charge” of the electric vehicle. Constraint (6) calculates the remaining electricity in battery for user i at the end of time t ($t \neq 1$), which equals the electricity in battery at the end of time $t - 1$ plus the energy drawn from the charging station at time t minus the energy consumption (due to driving) d_i^t during this one unit of time t . Note that x_i^t and d_i^t may not be positive at the same time because one does not charge and drive the vehicle simultaneously. Similarly, constraint (7) calculates the remaining electricity in battery for user i at the end of time $t=1$ based on the electricity in battery at the end of time T from the previous day. Constraint (8) states that the remaining electricity in battery for user i at any time does not exceed its capacity C , ensuring that the battery is not overcharged at all times. Constraint (9) assigns 1 to w_i^t and 0 to z_i^t whenever a new charge starts at time t during the day for user i , where T_s and T_e represent the start and end of the day-time charging periods, respectively. For example, if $T = 48$, then $T_s = 17$ (8am) and $T_e = 35$ (5pm). Similarly, constraint (10) ensures that when a new charge starts at the beginning of the day-time, it will be counted and $w_i^{T_s}$ is set to 1. Finally, constraint (11) specifies that variables x_i^t , u_i^t , w_i^t and z_i^t are all non-negative, while y_i^t is binary indicating if user i will charge or not at time interval t .

Note that in the most general setting when $p_t(v_t) = c_0^t + c^t v_t$ where $c^t \neq 0$ (i.e., unit price is a linear function of the total load), the OCS model is a quadratic mixed integer program. However, in a special case where $c^t = 0$ (e.g., ‘time-of-use’ rate), it reduces to a linear mixed integer program.

Finally, one variation of the OCS model is to allow users to charge for only a portion (e.g., half or quarter) of an assigned interval. This can be realized by changing (5) from equality constraint to its ‘ \leq ’ inequality counterpart. Obviously, this relaxation provides smaller optimal cost than does the original OCS model. However, the relaxation is likely to produce rather scattered charging profile, with high percentage of non-consecutive charging. Detailed numerical investigation of this tradeoff can be found in Chapter 4 Section 4.2.

Variable	Description
y_i^{total}	the total charging periods needed for user i
m_i	the charging periods needed during day-time for user i
n_i	the charging periods needed during night-time for user i
α	the energy drawn from the charging station during one unit of time
$amced_i$	the morning commute ending time for user i
$pmced_i$	the evening commute ending time for user i
$amcst_i$	the morning commute starting time for user i
a_i	the end of day-time charging for user i
b_i	the end of night-time charging for user i
D	the last possible time interval for day-time charging, e.g., $t = 35$

TABLE 1

Description of variables in Algorithm 1

3.2 A Rolling Horizon Heuristic (RHH) Algorithm

The centralized optimization model in Section 3.1 is implemented in GAMS/CPLEX and tested extensively. The numerical experience is that when the number of users, n , is large (e.g., 100), it becomes very difficult to solve the mixed integer model (OCS) to optimality using CPLEX. Thus, the rolling horizon heuristic is developed as an alternative solution method to provide good solutions quickly.

The principle of the rolling horizon heuristic (RHH) is to allocate the T time intervals evenly to all EV users. In order to fulfill an EV user’s daily charging demand, the RHH assigns half of the demand to be met during the day-time charging and the other half during the night-time charging. More specifically, the RHH starts from the first EV user, and assigns the first available day-time and night-time slots to this users’s day-time and night-time charge, respectively. Then the RHH schedules the second EV user’s charging, and so on. Whenever a user rolls to the end of day-time (8am-5pm) or night-time (5pm-8am) charging period, the RHH will search from the beginning of the period for the first available time slot and assign it to the user to fulfill his/her charging demand. This cycle repeats until all EV users’ charging is complete. The pseudo-code of the RHH method is given in Algorithm 1, which uses variables that are defined in Table 1.

Particularly, Algorithm 1 can be explained as follows. In Step 0, all y_i^t are

```

Step 0. (Initialization)
for  $i=1, n$  do
  |  $y_i^t = 0$ , for  $t \in 1, \dots, T$ . //  $T$  is the last time interval for the day, e.g.,  $T = 48$ 
end
Step 1. (calculate the charging periods needed during day-time ( $m_i$ ) and night-time ( $n_i$ ) for each user)
for  $i = 1, n$  do
  |  $y_i^{\text{total}} = d_i/\alpha$ ;  $m_i = \lfloor 0.5y_i^{\text{total}} \rfloor$ ;  $n_i = y_i^{\text{total}} - m_i$ 
end
Step 2. (assign charging periods for user 1)
   $y_1^t = 1$ , for  $\text{amced}_1 + 1 \leq t \leq \text{amced}_1 + m_1$  and  $\text{pmced}_1 + 1 \leq t \leq \text{pmced}_1 + n_1$ .
   $a_1 = \text{amced}_1 + m_1, b_1 = \text{pmced}_1 + n_1$ ; //  $a_1$  and  $b_1$  are the ends of the day and night charging
  for user 1, respectively
Step 3. (assign day-time charging periods for user  $i$  based on that for user  $i - 1$ )
for  $i=2, n$  do
  | if  $a_{i-1} + m_i \leq D - 1$  then
  | | //  $D$  is the last possible time interval for day-time charging, e.g.,  $D = 35$ 
  | | if  $a_{i-1} + 1 \geq \text{amced}_i$  then
  | | |  $y_i^t = 1$ , for  $a_{i-1} + 1 \leq t \leq a_{i-1} + m_i$ ;
  | | |  $a_i = a_{i-1} + m_i$ ;
  | | | else
  | | | |  $y_i^t = 1$ , for  $\text{amced}_i + 1 \leq t \leq \text{amced}_i + m_i$ ;
  | | | |  $a_i = \text{amced}_i + m_i$ ;
  | | | end
  | | //update  $a_i$ 
  | end
  | if  $a_{i-1} + m_i \geq D$  then
  | | if  $a_{i-1} + 1 \leq D - 1$  then
  | | |  $y_i^t = 1$ , for  $a_{i-1} + 1 \leq t \leq D - 1$ ;
  | | | end
  | |  $y_i^t = 1$ , for  $\text{amced}_i + 1 \leq t \leq \text{amced}_i + a_{i-1} + m_i - D + 1$ ;
  | |  $a_i = \text{amced}_i + a_{i-1} + m_i - D + 1$ ;
  | end
end
Step 4. (assign night-time charging periods for user  $i$  based on that for user  $i - 1$ )
for  $i = 2, n$  do
  | if ( $b_{i-1} + 1 \geq \text{pmced}_i + 1$  and  $b_{i-1} + n_i \leq T$ ) or ( $b_{i-1} + 1 \leq \text{amcst}_i - 1$  and
  |  $b_{i-1} + n_i \leq \text{amcst}_i - 1$ ) then
  | |  $y_i^t = 1$ , for  $b_{i-1} + 1 \leq t \leq b_{i-1} + n_i$ ;
  | |  $b_i = b_{i-1} + n_i$ ;
  | | //update  $b_i$ 
  | end
  | if  $b_{i-1} + 1 \geq \text{pmced}_i + 1$  and  $b_{i-1} + n_i \geq T$  then
  | | if  $b_{i-1} + 1 \leq T$  then
  | | |  $y_i^t = 1$ , for  $b_{i-1} + 1 \leq t \leq T$ ;
  | | | end
  | |  $y_i^t = 1$ , for  $1 \leq t \leq b_{i-1} + n_i - T$ ;
  | |  $b_i = b_{i-1} + n_i - T$ ;
  | end
  | if  $b_{i-1} + 1 \leq \text{amcst}_i - 1$  and  $b_{i-1} + n_i \geq \text{amcst}_i$  then
  | |  $y_i^t = 1$ , for  $b_{i-1} + 1 \leq t \leq \text{amcst}_i - 1$  and  $\text{pmced}_i + 1 \leq t \leq \text{pmced}_i + n_i - \text{amcst}_i + b_{i-1} + 1$ ;
  | |  $b_i = \text{pmced}_i + n_i - \text{amcst}_i + b_{i-1} + 1$ ;
  | end
  | if  $\text{amcst}_i \leq b_{i-1} + 1 \leq 35$  then
  | |  $y_i^t = 1$ , for  $\text{pmced}_i + 1 \leq t \leq \text{pmced}_i + n_i$ ;
  | |  $b_i = \text{pmced}_i + n_i$ ;
  | end
end

```

Algorithm 1 A Rolling horizon heuristic

initialized to be zero. In Step 1, the charging durations needed during day-time and night-time are calculated for each user. The daily demand for user i is divided equally into two halves and each half is met either through day-time or night-time charging. In Step 2, both the day-time and night-time charging periods for user 1 are assigned from the first available time intervals until user 1's demand is met. In Step 3, day-time charging periods for user i are assigned based on that for user $i - 1$. There are two different situations in this step. First, the assigned charging time intervals for user i end before the last possible time interval for day-time charging, D . If the assigned charging starting time intervals for user i begin after the morning commute ending time, then he/she should charge the vehicle following the previous user with m_i intervals. If the assigned charging starting time for user i begins before the morning commute ending time, then he/she should wait and start charging after the morning commute time with m_i intervals. Second, the assigned charging time intervals for user i end at or after D . If the assigned charging starting time for user i begins before D , then the user should start charging after user $i - 1$ until D . The rest of day-time charging demand of user i is met from time slots at the end of morning commute of user i , although this will coincide with other users' day-time charging. Finally in Step 3, after the assignment of user i 's day-time charging periods, a_i (the end of day-time charging for user i) is updated. In Step 4, the night-time charging periods for user i are assigned based on that for user $i - 1$.

The assignment of night-time charging in Step 4 is rather complex with four different situations. The first scenario is that the assigned night-time charging intervals for user i begin after the evening commute time and end before the last time interval for the day, or the assigned charging intervals begin and end before the morning commute starts. In other words, the whole night-charging period is either between the evening commute ending time and T or is between midnight and the morning commute starting time. Under this scenario, the user should charge the vehicle for n_i intervals following the completion of user $i - 1$. In the second scenario, the assigned night-time charging intervals for user i begin after the evening commute time and end after T . In this case, if the assigned charging starting time

for user i begins before T , then the user should start charging after the completion of user $i - 1$ until T . The rest of night-time charging demand will be met from time slots after midnight. The third scenario is where the assigned night-time charging intervals for user i begin before the morning commute time and end after that. The user should start charging after the completion of user $i - 1$ until the morning commuting starting time. The rest of night-time charging demand will be met from time slots after the evening commute ending time. The last scenario is when the assigned night-time charging intervals for user i begin after the morning commute time and end before D . The user should start charging the vehicle after the evening commute ending time for n_i intervals. After user i 's night-time charging is assigned in Step 4, b_i (the end of night-time charging for user i) is updated.

This rolling horizon heuristic is implemented and evaluated in the numerical experiments, and the results are discussed in Chapter 4 Section 4.2.

3.3 Decentralized Charging Heuristic

By definition, the decentralized charging scheduling means EV users, instead of a central controller, decide on when and how much to charge their vehicles. While the centralized model and algorithm in Section 3.1 can help a network controller to achieve the maximum load leveling via minimizing the total system-wide cost, there may be situations in the real world where a decentralized scheduling is more desirable by individuals. This Section focuses on the development of a decentralized charging scheduling heuristic.

Consider again the dynamic pricing where unit electricity price $p_t(v_t) = c_0^t + c^t v_t$ ($c^t \neq 0$) at time t is a linear function of the total load v_t at time t . Consequently, individuals' cost would depend on their own as well as others' charging schedule. Mathematically, recall that x_i^t and y_i^t are charging decision variables for user i at time t . Let \mathbf{X}_{-i}^t and \mathbf{Y}_{-i}^t be the charging scheduling vectors for all users other than i . Thus, given \mathbf{X}_{-i}^t and \mathbf{Y}_{-i}^t , user i fixes his/her charging schedule by solving the following subproblem:

$$(DCS-i) \quad \min_{x_i^t, y_i^t} f_i = \sum_{t=1}^T \tilde{p}_t(x_i^t; \mathbf{X}_{-i}^t) x_i^t + F \sum_t w_i^t \quad (12)$$

$$\text{s.t.} \quad \sum_{t=1}^T x_i^t = d_i, \quad (13)$$

$$\sum_{t \in \mathcal{C}_i} y_i^t = 0, \quad (14)$$

$$x_i^t = \alpha y_i^t, \quad \forall t \quad (15)$$

$$u_i^t = u_i^{t-1} + x_i^t - d_i^t, \quad t \geq 2 \quad (16)$$

$$u_i^1 = u_i^T + x_i^1 - d_i^1, \quad (17)$$

$$u_i^t \leq C, \quad \forall t \quad (18)$$

$$y_i^t - y_i^{t-1} = w_i^t - z_i^t, \quad T_s \leq t \leq T_e \quad (19)$$

$$y_i^{T_s} = w_i^{T_s}, \quad (20)$$

$$y_i^t \in \{0, 1\}, \quad x_i^t \geq 0, \quad u_i^t \geq 0, \quad w_i^t \geq 0, \quad z_i^t \geq 0, \quad \forall t, \quad (21)$$

where $\tilde{p}_t(x_i^t; \mathbf{X}_{-i}^t) = c_0^t + c^t(D_i^t + x_i^t + \sum_{j \neq i} (D_j^t + x_j^t))$ and D_i^t are as defined previously.

Note that x_i^t and y_i^t are the only decision variables in (DCS- i). In a sense, the original centralized model (OCS) decomposes to n subproblems (DCS- i). This motivates us to develop a distributed heuristic algorithm for solving these n subproblems simultaneously.

In essence, the method outlined in Algorithm 2 applies a ‘coordinate search’ in solving the OCS model in a distributed manner. Note that the linear cost function $\tilde{p}_t(x_i^t; \mathbf{X}_{-i}^t)$ in (DCS- i) is approximated by the average of historical prices from previous days, where \hat{p}_t is the approximate price. In addition, one may perceive that the iteration index l represents day l , and the algorithm settles on an ‘optimal’ charging schedule among users after a reasonable period (e.g., 30 days). On any given day l , users solve their own scheduling problem (DCS- i) and broadcast their ‘optimal’ charging profile in a serial manner. When all users complete their charging scheduling, the electricity price for the next day will be

Initialization:

$l \leftarrow 1$ and $\Delta \leftarrow \infty$ //set up the initial iteration index and solution gap;

$x(l)_i^t \leftarrow 0$ and $y(l)_i^t \leftarrow 0$ for all user i and time t ;

$\hat{p}(l)^t = c_0^t + c^t(\sum_{i=1}^n D_i^t)$ for all time t //set up initial price using household load only;

while $l < MaxIter$ and $\Delta > MaxGap$ **do**

step 1. Calculate an approximate price;

if $l > 1$ **then**

$\hat{p}^t = \frac{\sum_{k=1}^{l-1} \hat{p}(k)^t}{l-1}$ for all t ;

else

$\hat{p}^t = \hat{p}(l)^t$;

end

step 2. Calculate the charging profile for each user i sequentially ;

$i \leftarrow 1$;

while $i \leq n$ **do**

step 2.1. Solve (DCS- i) with the approximate \hat{p}^t replacing $\tilde{p}_t(x_i^t; \mathbf{X}_{-i}^t)$ for user i ;

step 2.2. Update $x(l)_i^t$ and $y(l)_i^t$;

step 2.3. Broadcast a control message to announce $x(l)_i$ to other users;

step 2.4. Update $\hat{p}^t = c_0^t + c^t(\sum_{j=1}^n D_j^t + \sum_{j=1}^i x(l)_j^t + \sum_{j=i+1}^n x^t(l-1)_j)$;

end

step 3. Update $\hat{p}(l)^t = \hat{p}^t(x(l)_1, x(l)_2, \dots, x(l)_n)$;

step 4. Update $\Delta = \|x(l)_i^t - x(l-1)_i^t\|$ and $l \leftarrow l + 1$;

end

return $x^{*t}_i = x(l)_i^t$ for all user i and time t ;

Algorithm 2 A coordinate search heuristic

adjusted based on today's final charging profiles among all users. The algorithm terminates when either the number of days exceeds a pre-specified limit $MaxIter$ or the gap between successive iterations is within the pre-specified tolerance $MaxGap$.

CHAPTER 4

NUMERICAL RESULTS

4.1 Data Generation

Because the current thesis focuses on BEVs only, the Nissan Leaf is chosen as a prototype 100% battery charged electric vehicle to evaluate the proposed models. According to Nissan USA [39], the Nissan Leaf is equipped with a 24 kWh lithium-ion battery and has a Depth of Discharge (DOD) of 80%. In addition, the Level 2 charger (240 V) is used as a prototype charging station, which is available to most BEV users and can charge up to 3.3 kWh of energy in one hour (see e.g., [39] and [40]). By using this charging facility, the Nissan Leaf is estimated to complete its charging in approximately 5.8 hours and can run roughly 100 miles with a full charged battery. Furthermore, as mentioned previously, short- and medium-distance EV users are considered in the thesis. Thus, short-distance users will need a maximum of approximately 6 hours for a complete charging while the medium-distance users will need a maximum of approximately 9 hours to fulfill the charging demand. The latter indicates that one full charge is not enough for the medium-distance users to complete their daily commute. Therefore, these users have to charge their EVs twice a day, once during the day time (at work) and once during the night time (at home). Finally, the total of 3.3 kWh per hour drawn from a level-2 charger implies a total of 1.65 kWh per half an hour. Hence, when implementing the centralized and decentralized models, $\alpha = 1.65$ in (OCS) and (DCS-*i*). Finally, our implementation of the linear cost function uses $c_0^t = 0.071$ and $c^t = 0.02$ [41] in $p_t(v_t) = c_0^t + c^t v_t$.

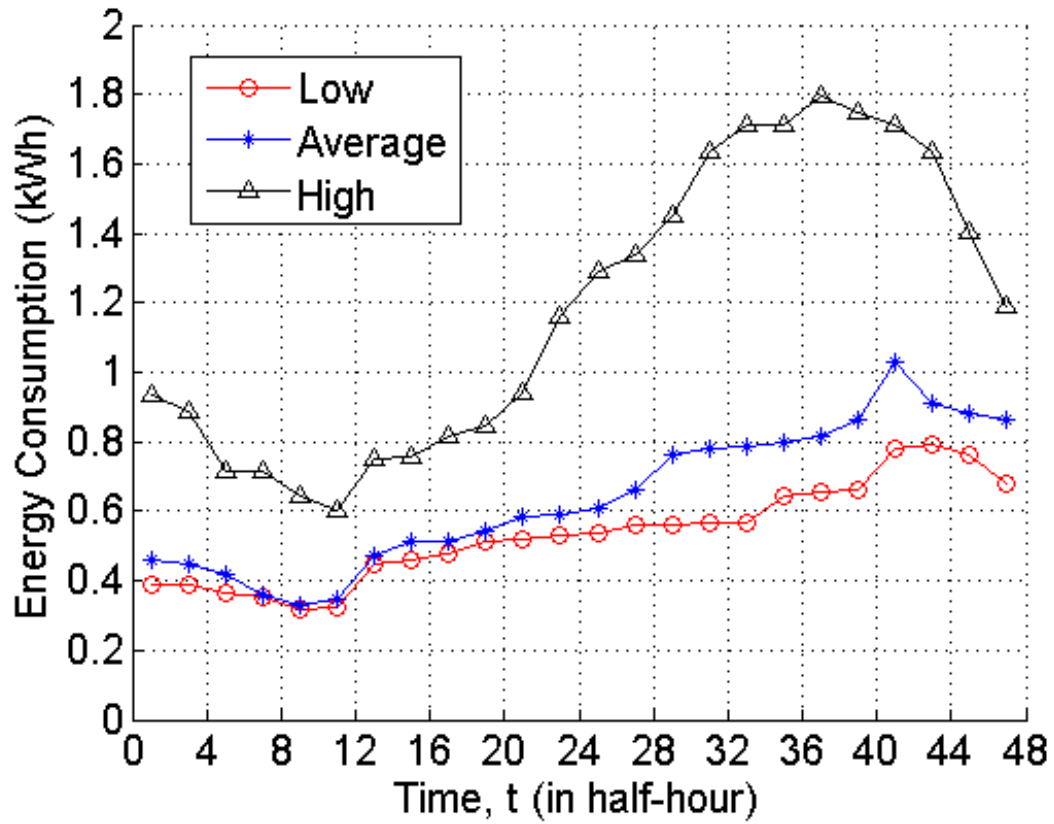


Figure 1. The household load profiles in summer months

In addition to the EV charging demand, the second source of electricity demand from the regular household usage is simulated based on studies reported by the Southern California Edison (SCE) territory [41]. In particular, household load profiles during the summer months (June, July, August and September) are used in the numerical experiments. Typically, the load profile of these summer months contains a single peak due to the increased electricity demand attributed to the hot weather. In addition, there are three categories of regular household load profiles: low-usage load profile with 23-28 kWh daily energy consumption, average-usage load profile with 29-36 kWh daily consumption, and high-usage load profile with 51-62 kWh daily consumption. Using this information and setting $T = 48$, a baseline household demand profile is randomly generated for half-hour duration (because $T = 48$) throughout a 24-hour cycle for the three types of users. Figure 1 illustrates the three prototypical baseline household demand profiles over 48

half-hour intervals. These randomly generated profiles exhibit the same peak and off-peak loads and periods as shown in the empirical data in [42].

Furthermore, in order to study the effectiveness of the proposed centralized and decentralized models, an uncontrolled charging profile is established as a benchmark. The uncontrolled charging scheduling assumes that when the system is left uncontrolled, the EV users will choose the most convenient time during evening hours between 5pm to 7am the following day to charge their vehicles. Starting times are randomly generated for the short and medium distance users. Once the charge starts, the uncontrolled charging solution lets users continue charging until the demand is fulfilled.

4.2 Results for OCS Models

The OCS model is implemented in GAMS, where the quadratic integer programs are solved by CPLEX 10.2. All experiments are run on a 16-core, dual Opteron server with 32 GB of memory and 13 TB of disk space in a RAID 6 configuration. The operating system is openSUSE 11 Linux. For all analysis, the total number of users, n , is varied with values 10, 50, 100 and 200. For each value of n , different penetration rates of medium-distance users, denoted as r , are tested using values of 20%, 35% and 50%. The fixed cost, fc , is also varied with fees \$0, \$0.25 and \$1. For each scenario with fixed values of n and fc , a total of 15 instances are run with 5 instances for each value of r . Then the average energy costs and the average peak-to-average ratios (PAR) are calculated for all 15 instances, where the PAR is calculated as $\frac{\text{maximum total load}}{\text{average total load}}$ for the entire system. These two measures are chosen because the centralized scheduling model is concerned with the overall performance of the entire distribution network. Another important measure is the percentage of non-consecutive charging (PNCC) during the day, calculated by $\frac{\text{total number of nonconsecutive charging during day-time}}{\text{total number of day-time charging intervals}}$ or $\frac{\sum_t w_i^t}{\sum_t y_i^t}$ for each user i . To some extent, PNCC shows how fixed setup cost will affect the continuity of day-time charging.

Instance	Penetration rate r											
	20%				35%				50%			
	f_{RLX}^* (\$)	UCI	f^* (\$)	UCI	f_{RLX}^* (\$)	UCI	f^* (\$)	UCI	f_{RLX}^* (\$)	UCI	f^* (\$)	UCI
1	145.98	28	146.28	8	144.78	27	145.13	7	159.20	28	159.65	9
2	139.91	28	140.18	7	151.47	28	151.75	8	152.92	28	153.63	8
3	141.42	28	141.74	7	146.24	27	146.42	7	159.72	28	160.45	9
4	141.96	28	142.32	7	153.63	28	154.35	8	165.22	28	165.40	9
5	148.26	28	148.81	7	147.36	28	147.69	8	160.37	28	160.84	9
Average	143.51	28	143.87	7	148.70	28	149.07	8	159.49	28	159.99	9

TABLE 2

Relaxation vs. original OCS model (linear cost, $n = 10$)

4.2.1 Models Vs. Linear Programming (LP) Relaxation

First, we investigate the tradeoff of allowing users to charge only for a portion of each assigned interval. We compute and count the average number of utilized charging intervals (UCI) for all 15 instances, where the UCI is counted for the entire system. As discussed previously, such a relaxation model is obtained by changing (5) from equality constraint to its “ \leq ” inequality counterpart in OCS model.

Tables 2 and 3 compare the relaxation and original models on a set of 5 instances for 10 and 100 users under linear cost, respectively. In both tables, column “ f_{RLX}^* ” gives the optimal cost of the relaxation model and column “ f^* ” provides that of the original model. Overall, in terms of total cost, both tables suggest that the advantage of the relaxation model over the original model is very marginal (in the order of 0.1%). Further, when comparing Tables 2 and 3, we observe that the advantage of the relaxation model diminishes as the number of users increases from 10 to 100. In particular, the average cost reduction due to the relaxation decreases from 0.27% for $n = 10$, to 0.01% for $n = 100$. On the other hand, in terms of UCI, both tables show significant disadvantage of the relaxation model over the original model. The average UCI increases from 8 to 28, which is a 250% growth for both $n = 10$ and $n = 100$. Due to the above observations, we drop the relaxation model from further consideration.

4.2.2 Results for MIP Models vs. Uncontrolled EV Charging

Table 4 displays the performance measures for uncontrolled charging for $n = 10$ users. From Table 4, we observe that the average energy cost is \$175.81 at

Instance	Penetration rate r											
	20%				35%				50%			
	f_{RLX}^* (\$)	UCI	f^* (\$)	UCI	f_{RLX}^* (\$)	UCI	f^* (\$)	UCI	f_{RLX}^* (\$)	UCI	f^* (\$)	UCI
1	10,586.03	28	10,586.70	7	11,846.03	28	11,846.35	8	12,755.13	28	12,755.69	9
2	10,577.28	28	10,577.90	7	11,659.38	28	11,659.72	8	12,485.68	28	12,485.88	9
3	11,151.60	28	11,152.42	7	11,680.18	28	11,681.47	8	12,553.74	28	12,554.35	9
4	10,631.54	28	10,631.94	7	11,405.56	28	11,406.74	8	12,274.99	28	12,275.34	9
5	11,164.42	28	11,165.20	7	11,521.74	28	11,522.69	8	12,566.92	28	12,567.55	9
Average	10,822.18	28	10,822.83	7	11,622.58	28	11,623.39	8	12,527.29	28	12,527.76	9

TABLE 3

Relaxation vs. original OCS model (linear cost, $n = 100$)

Instance	Penetration rate r					
	20%		35%		50%	
	Energy cost (\$)	PAR	Energy cost (\$)	PAR	Energy cost (\$)	PAR
1	180.38	2.29	175.96	2.31	194.14	2.32
2	169.66	2.51	183.16	2.39	181.40	2.27
3	174.93	2.51	179.56	2.50	197.35	2.34
4	168.81	2.09	187.96	2.31	201.32	2.30
5	185.29	2.33	178.92	2.47	194.36	2.35
Average	175.81	2.35	181.11	2.39	193.71	2.32

TABLE 4

Results for uncontrolled charging with the linear cost ($n = 10$)

20% penetration rate of medium-distance users. The average PAR, on the other hand, is calculated to be 2.35. As we increase the medium-distance penetration rate to 35%, the average energy cost increases slightly to \$181.11 while the average PAR increases to 2.39. Finally, at 50% penetration rate, the average energy cost is \$193.71 for 10 users with a PAR of 2.32. Overall, as the penetration rate of medium-distance users increases, the total electricity cost increases. However, the PAR shows no correlation with the penetration rate. Similar observations on the same five instances can be made from the results of the optimal charging with \$0, \$0.25 and \$1 fixed cost scenarios in Tables 5 to 7, respectively. Most importantly, when comparing the four tables, one observes that the average energy cost and PAR have been reduced considerably by all fixed cost scenarios in Tables 5 to 7. For example, at 20% penetration rate, the average energy cost reduces to \$143.50, \$143.69 and \$144.51 for \$0, \$0.25 and \$1 fixed cost scenarios, respectively. Similar observations can be made for $n=50$, 100 and 200 as shown in Tables 8 to 19.

Instance	Penetration rate r								
	20%			35%			50%		
	Energy cost (\$)	PNCC	PAR	Energy cost (\$)	PNCC	PAR	Energy cost (\$)	PNCC	PAR
1	145.91	0.91	1.10	144.78	0.82	1.10	159.09	0.87	1.20
2	139.95	0.93	1.14	151.22	0.84	1.14	152.99	0.90	1.12
3	141.32	0.94	1.13	146.02	0.83	1.11	159.84	0.76	1.12
4	141.96	0.91	1.11	153.81	0.82	1.21	165.21	0.86	1.10
5	148.39	0.85	1.25	147.54	0.76	1.24	160.49	0.83	1.11
Average	143.50	0.91	1.15	148.67	0.81	1.16	159.52	0.84	1.13

TABLE 5

Results for optimal charging with \$0 fixed cost ($n = 10$)

Instance	Penetration rate r								
	20%			35%			50%		
	Energy cost (\$)	PNCC	PAR	Energy cost (\$)	PNCC	PAR	Energy cost (\$)	PNCC	PAR
1	146.28	0.17	1.14	145.17	0.17	1.19	159.26	0.21	1.16
2	140.35	0.17	1.14	151.49	0.18	1.15	153.33	0.17	1.16
3	141.45	0.18	1.13	146.18	0.18	1.17	159.87	0.22	1.12
4	142.11	0.18	1.11	153.95	0.17	1.12	165.28	0.19	1.16
5	148.28	0.19	1.12	147.65	0.18	1.20	160.62	0.14	1.15
Average	143.69	0.18	1.13	148.89	0.18	1.17	159.67	0.19	1.15

TABLE 6

Results for optimal charging with \$0.25 fixed cost ($n = 10$)

Instance	Penetration rate r								
	20%			35%			50%		
	Energy cost (\$)	PNCC	PAR	Energy cost (\$)	PNCC	PAR	Energy cost (\$)	PNCC	PAR
1	146.60	0.11	1.20	144.89	0.10	1.16	159.23	0.14	1.11
2	141.23	0.09	1.17	152.33	0.09	1.19	153.21	0.14	1.11
3	142.30	0.10	1.18	146.70	0.10	1.17	159.94	0.14	1.14
4	142.45	0.14	1.16	155.02	0.12	1.16	165.40	0.12	1.13
5	149.95	0.10	1.17	148.04	0.10	1.16	160.78	0.13	1.15
Average	144.51	0.11	1.18	149.40	0.10	1.17	159.71	0.13	1.13

TABLE 7

Results for optimal charging with \$1 fixed cost ($n = 10$)

In order to evaluate OCS solutions, Table 20 compares the performance measures for uncontrolled charging and the OCS solution with $fc = \$0$, and Table 21 compares OCS solutions with $fc = \$0.25$ and those with $fc = \$1$. For each combination of (n, r) , i.e., the number of EV users and the penetration rate of medium-distance users, the energy cost and PAR reported in both tables are the averages over 5 instances. Overall, these results indicate that the proposed OCS model yields significant reduction in the energy cost as well as the PAR, when compared to uncontrolled charging scenario. For example, when $n=10$ and $r=20\%$, the OCS model with $fc = \$0$ reduces the energy cost and PAR from \$175.81 to \$143.50 (i.e., 18.38% improvement), and from 2.35 to 1.15 (i.e., 51.06% improvement), respectively. Furthermore, even with the highest fixed cost of \$1, the OCS model provides significant improvement over the uncontrolled scenario. In the previous example where $n=10$ and $r=20\%$, the OCS optimal charging model with \$1 fixed cost provides an improvement of 17.80% in the energy cost and 49.79% in the PAR.

4.2.3 Results for MIP Solutions for Various Fixed Setup Costs

When comparing OCS solutions with different setup costs, it can be observed from Table 5 to Table 7 that the PNCC decreases dramatically with the increase of the fixed cost. For example, when $n=10$, the PNCC is 0.91 for optimal charging with \$0 fixed cost at 20% penetration rate, and it significantly decreases to 0.18 for optimal charging with \$0.25 fixed cost at the same penetration rate, and 0.11 for optimal charging with \$1 fixed cost. This indicates that the application of the fixed cost can significantly reduce the non-consecutive charging during the day-time.

Similar observations can be made for $n=50, 100$ and 200 as shown in Tables 8 to 19.

In addition, we observe the following from Tables 20 and 21. First, collectively the two tables show that the energy cost increases when fc increases from zero to a non-zero value. This is because the OCS model with $fc = \$0$ minimizes the energy cost, while the OCS model with $fc \neq 0$ minimizes the sum of the energy and setup costs. Second, from Table 21, when fc increases from \$0.25 to

Instance	Penetration rate r					
	20%		35%		50%	
	Energy cost (\$)	PAR	Energy cost (\$)	PAR	Energy cost (\$)	PAR
1	3,645.87	2.42	3,949.04	2.38	3,976.36	2.30
2	3,440.53	2.48	3,820.17	2.40	4,094.93	2.27
3	3,382.58	2.32	3,665.51	2.43	3,989.71	2.29
4	3,560.23	2.47	3,709.04	2.24	3,981.33	2.35
5	3,599.80	2.40	3,936.65	2.30	4,101.53	2.28
Average	3,525.80	2.42	3,816.08	2.35	4,028.77	2.30

TABLE 8

Results for uncontrolled charging with the linear cost ($n = 50$)

Instance	Penetration rate r								
	20%			35%			50%		
	Energy cost (\$)	PNCC	PAR	Energy cost (\$)	PNCC	PAR	Energy cost (\$)	PNCC	PAR
1	2,831.53	0.82	1.07	3,084.23	0.88	1.04	3,186.24	0.83	1.05
2	2,726.42	0.88	1.10	3,001.10	0.83	1.05	3,218.14	0.81	1.05
3	2,714.36	0.87	1.14	2,910.42	0.87	1.06	3,204.34	0.81	1.08
4	2,777.86	0.90	1.09	2,978.52	0.82	1.06	3,193.71	0.83	1.04
5	2,809.55	0.84	1.07	3,082.67	0.80	1.07	3,270.10	0.82	1.03
Average	2,771.95	0.86	1.09	3,011.39	0.84	1.06	3,214.50	0.82	1.05

TABLE 9

Results for optimal charging with \$0 fixed cost ($n = 50$)

Instance	Penetration rate r								
	20%			35%			50%		
	Energy cost (\$)	PNCC	PAR	Energy cost (\$)	PNCC	PAR	Energy cost (\$)	PNCC	PAR
1	2,832.46	0.33	1.08	3,085.29	0.22	1.06	3,187.07	0.26	1.07
2	2,778.01	0.32	1.09	3,001.61	0.30	1.06	3,218.96	0.27	1.06
3	2,715.75	0.32	1.14	2,911.79	0.18	1.08	3,205.38	0.28	1.07
4	2,778.01	0.19	1.09	2,995.92	0.25	1.27	3,194.49	0.27	1.11
5	2,810.17	0.23	1.07	3,083.17	0.22	1.05	3,270.81	0.23	1.06
Average	2,782.88	0.28	1.09	3,015.56	0.23	1.10	3,215.34	0.26	1.07

TABLE 10

Results for optimal charging with \$0.25 fixed cost ($n = 50$)

Instance	Penetration rate r								
	20%			35%			50%		
	Energy cost (\$)	PNCC	PAR	Energy cost (\$)	PNCC	PAR	Energy cost (\$)	PNCC	PAR
1	2,834.88	0.19	1.07	3,086.94	0.17	1.06	3,188.80	0.19	1.07
2	2,727.48	0.20	1.10	3,004.39	0.14	1.06	3,220.08	0.18	1.10
3	2,717.18	0.22	1.14	2,912.47	0.18	1.06	3,207.00	0.20	1.07
4	2,779.85	0.17	1.09	2,983.49	0.22	1.12	3,197.48	0.22	1.08
5	2,814.16	0.25	1.09	3,086.05	0.14	1.07	3,273.35	0.20	1.06
Average	2,774.71	0.21	1.10	3,014.67	0.17	1.07	3,217.34	0.20	1.08

TABLE 11

Results for optimal charging with \$1 fixed cost ($n = 50$)

Instance	Penetration rate r					
	20%		35%		50%	
	Energy cost (\$)	PAR	Energy cost (\$)	PAR	Energy cost (\$)	PAR
1	13,375.02	2.43	15,108.24	2.31	16,225.92	2.28
2	13,504.93	2.50	14,821.39	2.36	15,931.61	2.24
3	14,556.88	2.44	14,894.92	2.36	15,817.94	2.26
4	13,512.11	2.39	14,372.83	2.38	15,253.63	2.26
5	14,554.22	2.42	14,532.80	2.34	15,745.56	2.30
Average	13,900.63	2.44	14,746.04	2.35	15,794.93	2.27

TABLE 12

Results for uncontrolled charging with the linear cost ($n = 100$)

Instance	Penetration rate r								
	20%			35%			50%		
	Energy cost (\$)	PNCC	PAR	Energy cost (\$)	PNCC	PAR	Energy cost (\$)	PNCC	PAR
1	10,586.35	0.86	1.09	11,846.43	0.82	1.04	12,755.42	0.84	1.03
2	10,578.11	0.89	1.09	11,660.08	0.83	1.05	12,485.64	0.83	1.03
3	11,152.05	0.88	1.06	11,680.56	0.84	1.03	12,554.38	0.83	1.04
4	10,632.04	0.85	1.08	11,405.98	0.87	1.05	12,275.54	0.82	1.04
5	11,164.86	0.84	1.06	11,522.35	0.84	1.04	12,567.72	0.84	1.03
Average	10,822.68	0.86	1.07	11,623.08	0.84	1.04	12,527.74	0.83	1.04

TABLE 13

Results for optimal charging with \$0 fixed cost ($n = 100$)

Instance	Penetration rate r								
	20%			35%			50%		
	Energy cost (\$)	PNCC	PAR	Energy cost (\$)	PNCC	PAR	Energy cost (\$)	PNCC	PAR
1	10,586.94	0.20	1.09	11,846.61	0.23	1.03	12,756.05	0.23	1.04
2	10,581.25	0.19	1.09	11,660.55	0.20	1.05	12,486.65	0.22	1.03
3	11,152.37	0.20	1.06	11,681.05	0.18	1.03	12,555.04	0.23	1.04
4	10,632.62	0.26	1.08	11,406.48	0.26	1.05	12,275.30	0.24	1.03
5	11,166.18	0.19	1.06	11,522.54	0.21	1.04	12,568.78	0.19	1.05
Average	10,823.87	0.21	1.07	11,623.45	0.22	1.04	12,528.37	0.22	1.04

TABLE 14

Results for optimal charging with \$0.25 fixed cost ($n = 100$)

Instance	Penetration rate r								
	20%			35%			50%		
	Energy cost (\$)	PNCC	PAR	Energy cost (\$)	PNCC	PAR	Energy cost (\$)	PNCC	PAR
1	10,589.74	0.17	1.09	11,852.83	0.19	1.08	12,762.60	0.22	1.12
2	10,580.56	0.17	1.09	11,665.14	0.25	1.07	12,504.59	0.21	1.15
3	11,155.82	0.18	1.06	11,685.51	0.22	1.06	12,561.77	0.22	1.08
4	10,634.95	0.21	1.08	11,412.36	0.21	1.05	12,281.25	0.20	1.05
5	11,168.47	0.18	1.06	11,526.26	0.21	1.04	12,575.01	0.21	1.05
Average	10,825.91	0.18	1.07	11,628.42	0.22	1.06	12,537.04	0.21	1.09

TABLE 15

Results for optimal charging with \$1 fixed cost ($n = 100$)

Instance	Penetration rate r					
	20%		35%		50%	
	Energy cost (\$)	PAR	Energy cost (\$)	PAR	Energy cost (\$)	PAR
1	54,542.03	2.39	57,442.56	2.33	61,565.03	2.28
2	54,124.27	2.43	59,333.19	2.34	61,084.34	2.31
3	55,081.06	2.43	58,963.92	2.34	61,383.03	2.29
4	53,797.21	2.43	58,271.08	2.33	61,369.27	2.27
5	54,941.72	2.42	57,502.56	2.34	63,218.80	2.30
Average	54,497.26	2.42	58,302.66	2.34	61,724.10	2.29

TABLE 16

Results for uncontrolled charging with the linear cost ($n = 200$)

Instance	Penetration rate r								
	20%			35%			50%		
	Energy cost (\$)	PNCC	PAR	Energy cost (\$)	PNCC	PAR	Energy cost (\$)	PNCC	PAR
1	42,647.78	0.88	1.08	45,261.59	0.80	1.05	48,914.17	0.78	1.03
2	42,342.72	0.87	1.09	46,392.72	0.84	1.03	48,486.52	0.76	1.03
3	42,609.14	0.87	1.09	46,157.85	0.78	1.04	48,955.19	0.79	1.03
4	42,042.00	0.82	1.08	45,999.05	0.79	1.03	48,396.31	0.81	1.02
5	42,740.20	0.87	1.08	45,344.85	0.85	1.05	49,680.87	0.79	1.02
Average	42,476.37	0.86	1.08	45,831.21	0.81	1.04	48,886.61	0.79	1.03

TABLE 17

Results for optimal charging with \$0 fixed cost ($n = 200$)

Instance	Penetration rate r								
	20%			35%			50%		
	Energy cost (\$)	PNCC	PAR	Energy cost (\$)	PNCC	PAR	Energy cost (\$)	PNCC	PAR
1	42,648.96	0.24	1.08	45,260.97	0.21	1.05	48,915.48	0.23	1.03
2	42,343.26	0.21	1.09	46,398.85	0.23	1.05	48,488.27	0.23	1.03
3	42,612.30	0.22	1.09	46,158.73	0.21	1.04	48,957.86	0.20	1.03
4	42,042.53	0.21	1.08	45,999.77	0.24	1.03	48,397.91	0.22	1.03
5	42,742.26	0.21	1.08	45,346.36	0.23	1.05	49,681.95	0.20	1.02
Average	42,477.86	0.22	1.08	45,832.94	0.22	1.04	48,888.29	0.22	1.03

TABLE 18

Results for optimal charging with \$0.25 fixed cost ($n = 200$)

Instance	Penetration rate r								
	20%			35%			50%		
	Energy cost (\$)	PNCC	PAR	Energy cost (\$)	PNCC	PAR	Energy cost (\$)	PNCC	PAR
1	42,651.82	0.19	1.08	45,265.59	0.26	1.05	48,921.21	0.20	1.04
2	42,352.32	0.22	1.09	46,397.30	0.23	1.03	48,509.84	0.24	1.10
3	42,615.06	0.20	1.09	46,167.27	0.20	1.04	48,961.79	0.28	1.04
4	42,046.51	0.20	1.08	46,011.35	0.22	1.05	48,406.09	0.21	1.05
5	42,744.86	0.21	1.08	45,350.54	0.20	1.05	49,692.41	0.19	1.03
Average	42,482.11	0.20	1.08	45,838.41	0.22	1.04	48,898.27	0.22	1.05

TABLE 19

Results for optimal charging with \$1 fixed cost ($n = 200$)

n	r	Uncontrolled		fc=\$0		
		Energy cost (\$)	PAR	Energy cost (\$)	PNCC	PAR
10	20%	175.81	2.35	143.50	0.91	1.15
	35%	181.11	2.39	148.67	0.81	1.16
	50%	193.71	2.32	159.52	0.84	1.13
50	20%	3,525.80	2.42	2,771.95	0.86	1.09
	35%	3,816.08	2.35	3,011.39	0.84	1.06
	50%	4,028.77	2.30	3,214.50	0.82	1.05
100	20%	13,900.63	2.44	10,822.68	0.86	1.07
	35%	14,746.04	2.35	11,623.08	0.84	1.04
	50%	15,794.93	2.27	12,527.74	0.83	1.04
200	20%	54,497.26	2.42	42,476.37	0.86	1.08
	35%	58,302.66	2.34	45,831.21	0.81	1.04
	50%	61,724.10	2.29	48,886.61	0.79	1.03

TABLE 20

Results of the (OCS) using the linear cost function (Uncontrolled and fc = \$0)

n	r	fc=\$0.25			fc=\$1		
		Energy cost (\$)	PNCC	PAR	Energy cost (\$)	PNCC	PAR
10	20%	143.69	0.18	1.13	144.51	0.11	1.18
	35%	148.89	0.18	1.17	149.40	0.10	1.17
	50%	159.67	0.19	1.15	159.71	0.13	1.13
50	20%	2,782.88	0.28	1.09	2,774.71	0.21	1.10
	35%	3,015.56	0.23	1.10	3,014.67	0.17	1.07
	50%	3,215.34	0.26	1.07	3,217.34	0.20	1.08
100	20%	10,823.87	0.21	1.07	10,825.91	0.18	1.07
	35%	11,623.45	0.22	1.04	11,628.42	0.22	1.06
	50%	12,528.37	0.22	1.04	12,537.04	0.21	1.09
200	20%	42,477.86	0.22	1.08	42,482.11	0.20	1.08
	35%	45,832.94	0.22	1.04	45,838.41	0.22	1.04
	50%	48,888.29	0.22	1.03	48,898.27	0.22	1.05

TABLE 21

Results of the (OCS) using the linear cost function (fc = \$0.25 and fc = \$1)

\$1, the energy cost for $fc=\$1$ is not necessarily larger than that for $fc=\$0.25$. For example, the energy cost for $n = 50$, $r = 20\%$ and $fc = 1$ is \$2,774.71, lower than that for $n = 50$, $r = 20\%$ and $fc = \$0.25$. This is again because in both scenarios ($fc = \$0.25$ and $fc = \$1$), OCS minimizes the total energy and setup costs and the energy cost may not exhibit any patterns between the two settings. Third, Tables 20 and 21 indicate that an OCS model with a non-zero fc can significantly reduce the percentage of non-consecutive charge (PNCC) without notable increase in the energy cost and PAR. For example, when $n=10$ and $r=20\%$, the scenario of $fc=\$0.25$ provides an approximate 80% improvement in the PNCC, when compared to the scenario of $fc = \$0$. For the case of $fc=\$1$, the improvement on PNCC is roughly 88% improvement. This shows that including the setup cost in the OCS model is extremely valuable in reducing PNCC without much sacrifice on PAR and the energy cost.

Overall, the OCS model offers greater flexibility in the day-time charging (between 8am to 5pm) when the baseline household demand is low. Thus, the user would shift the load for EV charging to the periods of low energy consumption. Consequently, the energy cost is reduced and the total energy demand is distributed more evenly with a reduced PAR.

Figure 2 displays the charging profile for a medium-distance EV user (user 1, whose EV demand is 26.4 kWh) in four charging scenarios. Figure 2(a) shows the charging profile when the user is left uncontrolled. In this case, user 1 starts charging at 7pm ($t = 39$) and completes his/her charging by 3am ($t = 7$) the following day, using a total of 16 half-hour intervals. Figure 2(b) depicts user 1's optimal charging profile from the OCS with $fc = 0$, which has several separate and disjoint charging periods during the day. The allocation of these charging periods given by the central controller is based on the price at the specific time such that all users' total cost is minimized. Figure 2(c) shows the optimal charging profile for user 1 from the OCS with $fc = 0.25$. It can be observed that user 1 is assigned to charge the vehicle from 8am ($t = 17$) to 11am ($t = 23$) and from 12:30pm ($t = 26$) to 1pm ($t = 27$). The whole day-time charging of 7 half-hour intervals is divided

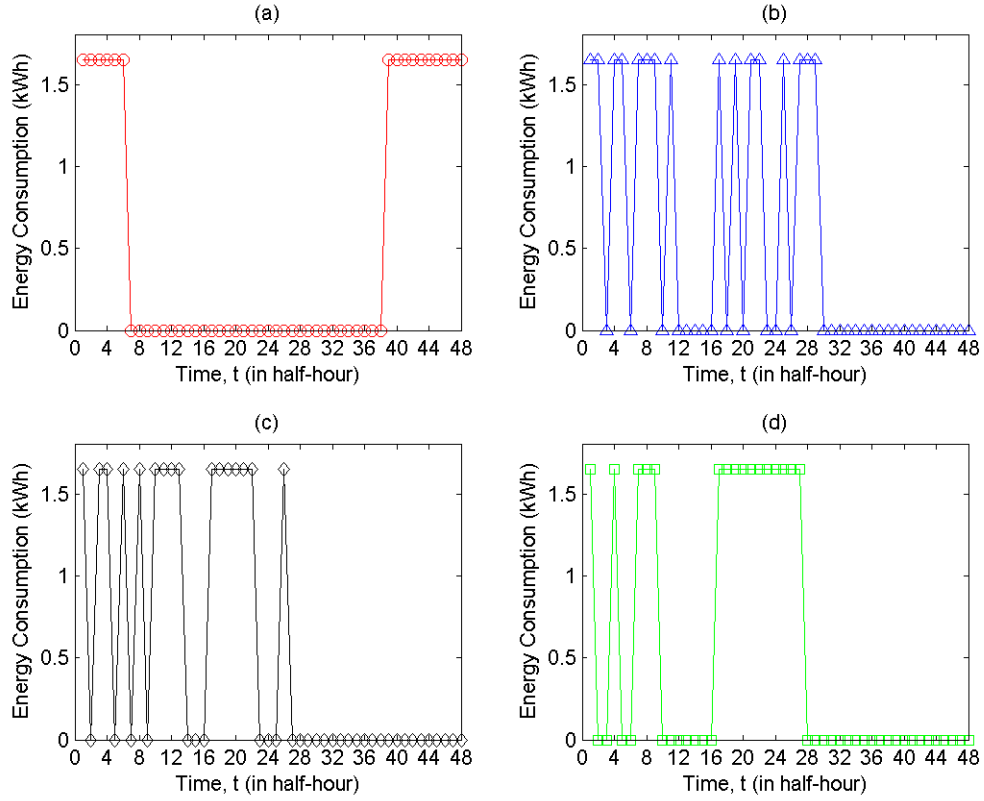


Figure 2. Four scenarios of charging profile for user 1 under uncontrolled and OCS model

into two sections. Finally, Figure 2(d) illustrates the optimal charging profile for user 1 from the OCS with $f_c = 1$. Compared to uncontrolled (in Figure 2(a)), zero fixed cost optimal charging (in Figure 2(b)) and \$0.25 fixed cost optimal charging (in Figure 2(c)), this charging profile has a total of 5.5 consecutive charging hours (or 11 consecutive half hour intervals) during the day between 8am ($t = 17$) to 1:30pm ($t = 28$), thus drawing a total of 18.15 kWh of energy. Nonetheless, the charging schedule during the evening hours is not subject to the fixed setup cost. Therefore, in Figure 2(d), user 1 is scheduled to charge for only one interval at 12am, and to charge for four consecutive intervals from 3:30am to 5:30am.

Figure 3 illustrates a comparison of load leveling achieved through four charging scenarios, uncontrolled charging scenario (the ‘o’ series), the OCS model with zero fixed cost (the ‘ Δ ’ series), the OCS model with \$0.25 fixed cost (the ‘ \diamond ’

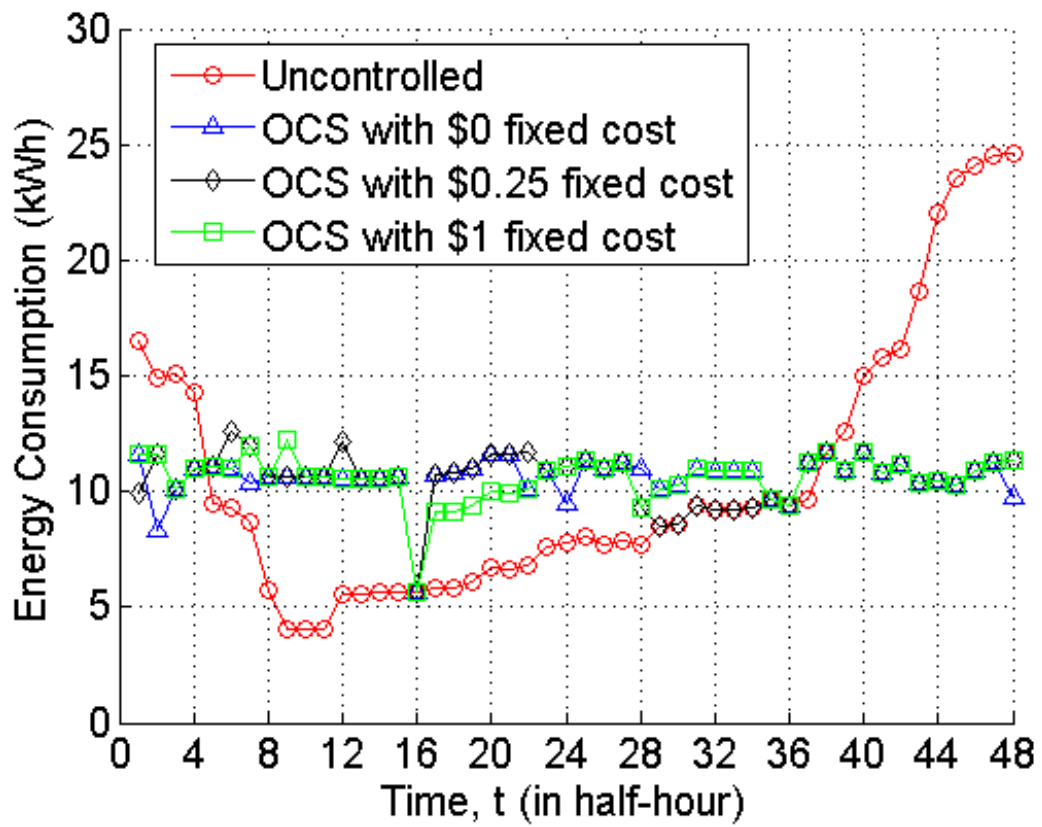


Figure 3. Overall load leveling under uncontrolled charging and (OCS) model with different fixed cost ($n=10$)

series) and the OCS model with \$1 fixed cost (the ‘*’ series) for the case of $n = 10$ users. The vertical axis is the total load of regular household usage and EV charging from all 10 users. Several observations are made from this figure. First, the load profile for the uncontrolled charging scenario demonstrates a significant demand peak between $t = 37$ (6pm) and $t = 3$ (1am the following day), and a demand valley between $t = 8$ (3:30am) and $t = 36$ (5:30pm). Second, all three optimal charging scenarios help flatten the load curve by reducing the evening peak by more than 50%, but with demand valleys at $t = 16$ (7:30 am) due to the morning commute and at $t = 35$ to 36 due to the evening commute. Finally, the OCS models with $fc = \$0.25$ and $fc = \$1$ provide almost the same load leveling effect as the OCS model with $fc = \$0$. Thus, it is concluded that the OCS model with high fixed costs significantly reduces the PNCC without notable losses on energy cost, PAR and load leveling.

4.3 Results for Rolling Horizon Heuristic (RHH)

Table 22 displays the total CPU time used by CPLEX 10.2 to solve the OCS models. First, for a fixed value of n , when the setup cost increases from zero to non-zero, the CPU time required for solving the OCS model increases significantly. For example, when $n = 50$, the average CPU time for $fc = \$0$ is 1.13 seconds, for $fc = \$0.25$ is 345.26 seconds (a 300 folds increase) and for $fc = \$1$ is 634.16 seconds (a 600 folds increase). Second, as the number of EV users increases, the average CPU time increases and reaches to an average of approximately 30 minutes when $n = 200$. This motivates the development of the proposed rolling horizon heuristic (RHH) method, which uses negligible CPU time in solving the charging scheduling problem. The RHH is also implemented in GAMS and the following table compares the solution quality of the RHH method with that of the OCS model by CPLEX 10.2.

Specifically, Table 23 compares the energy cost of the RHH solution with that of various OCS solutions. For each combination of (n, r) , the energy cost of the RHH solution is reported in the third column; and the fourth column displays the energy

n	r	CPU time (sec)		
		fc = \$0	fc = \$0.25	fc = \$1
10	20%	0.09	7.42	28.24
	35%	0.09	8.81	12.21
	50%	0.09	8.36	85.31
	Average	0.09	8.19	41.92
50	20%	1.05	104.61	454.67
	35%	1.10	576.33	515.49
	50%	1.24	354.84	932.31
	Average	1.13	345.26	634.16
100	20%	4.19	1,041.73	1,262.15
	35%	4.18	311.51	190.05
	50%	4.71	299.55	224.63
	Average	4.36	550.93	558.94
200	20%	15.89	1,881.92	1,399.87
	35%	218.12	1,760.14	1,298.26
	50%	504.43	1,956.88	1,721.54
	Average	246.15	1,866.31	1,473.22

TABLE 22

CPU times for (OCS) charging scenarios

n	r	Energy cost of rolling heuristic (\$)	fc = \$0		fc = \$0.25		fc = \$1	
			Energy cost (\$)	Gap %	Energy cost (\$)	Gap %	Energy cost (\$)	Gap %
10	20%	149.84	143.50	4.41	143.69	4.28	144.51	3.69
	35%	154.94	148.67	4.21	148.89	4.06	149.40	3.71
	50%	167.04	159.52	4.71	159.67	4.61	159.71	4.59
50	20%	2,922.13	2,771.95	5.42	2,782.88	5.00	2,774.71	5.31
	35%	3,168.29	3,011.39	5.21	3,015.56	5.06	3,014.67	5.10
	50%	3,383.20	3,214.50	5.25	3,215.34	5.22	3,217.34	5.15
100	20%	11,406.26	10,822.68	5.39	10,823.87	5.38	10,825.91	5.36
	35%	12,235.44	11,623.08	5.27	11,623.45	5.27	11,628.42	5.22
	50%	13,176.32	12,527.74	5.18	12,528.37	5.17	12,537.04	5.10
200	20%	44,796.44	42,476.37	5.46	42,477.86	5.46	42,482.11	5.45
	35%	48,255.00	45,831.21	5.29	45,832.94	5.28	45,838.41	5.27
	50%	51,425.44	48,886.61	5.19	48,888.29	5.19	48,898.27	5.17
Average			—	5.08	—	5.00	—	4.93

TABLE 23

Results of rolling heuristic and comparison with (OCS) charging scenarios

cost of the OCS solution with $fc = \$0$ and the gap between these two energy costs. The gap is calculated as $\frac{\text{energy cost of rolling heuristic} - \text{energy cost of (OCS) scenario}}{\text{energy cost of (OCS) scenario}} \times 100\%$. Similar information is provided for the OCS solutions with $fc = \$0.25$ and $fc = \$1$ in columns five and six, respectively. Note that all quantities reported in the table are the averages over 5 instances. It can be observed that the smallest gap is 3.69%, achieved at $n=10$, $r=20\%$ and $fc = \$1$. The highest gap is 5.46%, achieved at $n=200$, $r=20\%$ and $fc=\$0$ or $\$0.25$. Overall, across three values for fc and four values for n , the average optimality gap for the RHH is 5%. This shows that the RHH method is a good alternative to produce quality solutions in much less (indeed negligible) CPU time, when compared to the OCS model solved by general purpose solvers such as CPLEX.

4.4 Results for Decentralized Models

The decentralized coordinate search heuristic (Algorithm 2 of Section 3.3) is also implemented in GAMS/CPLEX, using the same random instances and linear cost function $\tilde{p}_t(x_i^t; \mathbf{X}_{-i}^t) = c_0^t + c^t(D_i^t + x_i^t + \sum_{j \neq i} (D_j^t + x_j^t))$ ($c_0^t = 0.071$ and $c^t = 0.02$) as in Section 4.2. *MaxIter* and *MaxGap* are set to be 100 and 0.01, respectively. In other words, users are allowed to learn the price dynamics over 100 days before the ‘optimal’ charging schedule is settled among all users.

Table 24 displays the performance measures for DCS model with $\$0$ fixed cost for $n = 10$ users. From Table 24, we observe that the average energy cost is $\$158.21$ at 20% penetration rate of medium-distance users. The average PAR, on the other hand, is calculated to be 1.97. As the medium-distance penetration rate increases to 35%, the average energy cost increases slightly to $\$159.63$ while the average PAR decreases to 1.91. Finally, at the 50% penetration rate, the average energy cost is $\$172.76$ for 10 users with a PAR of 1.88. Overall, as the penetration rate of medium-distance users increases, the total electricity cost increases. Similar observations of the energy cost on the same five instances can be made from the results of the DCS charging with $\$0.25$ and $\$1$ fixed cost scenarios in Tables 25 to 26, respectively. However, the PAR shows no correlation with the penetration rate.

Instance	Penetration rate r					
	20%		35%		50%	
	Energy cost (\$)	PAR	Energy cost (\$)	PAR	Energy cost (\$)	PAR
1	160.72	1.97	157.24	2.09	169.81	1.93
2	154.69	1.97	161.14	1.91	165.48	1.87
3	157.66	1.97	155.43	1.77	173.57	1.85
4	154.43	1.95	168.71	1.88	178.77	1.91
5	163.55	2.02	155.64	1.92	176.16	1.86
Average	158.21	1.97	159.63	1.91	172.76	1.88

TABLE 24

Results for decentralized charging with \$0 fixed cost ($n = 10$)

For Table 25, when the penetration rate of the medium-distance users increases from 20% to 35% to 50%, the average PAR increase from 1.30 to 1.37 to 1.55. However, in Table 26, when the penetration rate of the medium-distance users increases from 20% to 35% to 50%, the average PAR first increases from 1.31 to 1.95 then decrease to 1.85.

Most importantly, when comparing these three tables with the uncontrolled charging scenario in Table 4, one observes that the average energy cost and PAR have been reduced considerably in scenarios of various fixed costs in Tables 24 to 26. For example, at 20% penetration rate, the average energy cost reduces from \$175.81 (uncontrolled) to \$158.21 ($fc=\0), \$144.73 ($fc=\0.25) and \$146.95 ($fc=\1). Similar observations can be made for $n=50$, 100 and 200 as shown in Tables 27 to 35.

Another observation is that although for $n=10$, the lowest average energy cost is achieved at the scenario with \$0.25 fixed cost, it cannot be concluded that the DCS charging with \$0.25 provides the best solution for decentralized charging. For example, for $n=50$ and $r=20\%$, the lowest average energy cost is achieved at $fc=\$1$ with \$2,813.92. We speculate that this is because the DCS algorithm is only a heuristic model, which can provide a good feasible solution but not the optimal solution.

Figure 4 displays the detailed charging profile for a medium-distance EV user (user 1, whose EV demand is 26.4 kWh) in uncontrolled and three decentralized

Instance	Penetration rate r					
	20%		35%		50%	
	Energy cost (\$)	PAR	Energy cost (\$)	PAR	Energy cost (\$)	PAR
1	146.68	1.30	146.37	1.47	168.87	1.87
2	140.78	1.33	152.78	1.29	159.45	1.47
3	142.07	1.18	147.32	1.36	162.77	1.53
4	145.07	1.42	154.95	1.31	168.58	1.51
5	149.04	1.25	150.89	1.42	161.23	1.38
Average	144.73	1.30	150.46	1.37	164.18	1.55

TABLE 25

Results for decentralized charging with \$0.25 fixed cost ($n = 10$)

Instance	Penetration rate r					
	20%		35%		50%	
	Energy cost (\$)	PAR	Energy cost (\$)	PAR	Energy cost (\$)	PAR
1	148.21	1.31	155.32	1.94	169.32	1.87
2	144.55	1.50	160.79	1.98	162.10	1.90
3	142.87	1.48	156.60	1.96	169.83	1.84
4	147.77	1.82	164.59	1.96	173.88	1.83
5	151.37	1.61	160.22	1.92	167.86	1.82
Average	146.95	1.31	159.50	1.95	168.60	1.85

TABLE 26

Results for decentralized charging with \$1 fixed cost ($n = 10$)

Instance	Penetration rate r					
	20%		35%		50%	
	Energy cost (\$)	PAR	Energy cost (\$)	PAR	Energy cost (\$)	PAR
1	3184.83	1.96	3439.54	1.94	3510.22	1.94
2	3057.31	2.00	3296.58	1.91	3514.40	1.84
3	3049.86	2.00	3276.80	1.93	3442.66	1.86
4	3147.41	1.98	3221.63	1.94	3490.20	1.85
5	3176.42	1.97	3410.03	1.87	3568.86	1.84
Average	3123.17	1.96	3328.92	1.92	3505.27	1.87

TABLE 27

Results for decentralized charging with \$0 fixed cost ($n = 50$)

Instance	Penetration rate r					
	20%		35%		50%	
	Energy cost (\$)	PAR	Energy cost (\$)	PAR	Energy cost (\$)	PAR
1	2891.36	1.41	3158.66	1.31	3257.11	1.36
2	2784.57	1.47	3053.99	1.44	3284.69	1.33
3	2770.61	1.52	2974.71	1.46	3278.40	1.22
4	2842.05	1.37	3014.09	1.35	3269.10	1.50
5	2856.54	1.36	3134.17	1.29	3340.02	1.31
Average	2829.03	1.41	3067.12	1.37	3285.86	1.34

TABLE 28

Results for decentralized charging with \$0.25 fixed cost ($n = 50$)

Instance	Penetration rate r					
	20%		35%		50%	
	Energy cost (\$)	PAR	Energy cost (\$)	PAR	Energy cost (\$)	PAR
1	2875.16	1.26	3119.37	1.29	3255.28	1.42
2	2765.81	1.52	3035.92	1.29	3278.44	1.52
3	2760.45	1.33	2948.42	1.43	3286.30	1.55
4	2828.65	1.42	3007.94	1.27	3247.64	1.37
5	2839.54	1.42	3115.10	1.34	3302.50	1.29
Average	2813.92	1.26	3045.35	1.32	3274.03	1.43

TABLE 29

Results for decentralized charging with \$1 fixed cost ($n = 50$)

Instance	Penetration rate r					
	20%		35%		50%	
	Energy cost (\$)	PAR	Energy cost (\$)	PAR	Energy cost (\$)	PAR
1	11,918.93	2.00	13,057.98	1.89	14,104.78	1.81
2	11,998.30	1.99	12,774.25	1.90	14,069.75	1.84
3	12,541.14	1.95	13,143.43	2.07	13,706.91	1.86
4	11,887.55	2.02	12,606.24	2.02	13,401.89	1.88
5	12,733.12	1.94	12,802.88	2.01	13,282.17	1.83
Average	12,215.81	2.00	12,876.96	1.98	13,713.10	1.84

TABLE 30

Results for decentralized charging with \$0 fixed cost ($n = 100$)

Instance	Penetration rate r					
	20%		35%		50%	
	Energy cost (\$)	PAR	Energy cost (\$)	PAR	Energy cost (\$)	PAR
1	10,919.04	1.47	11,987.93	1.35	13,052.86	1.46
2	10,754.47	1.34	11,871.61	1.29	12,701.78	1.28
3	11,309.79	1.29	11,925.21	1.32	12,764.56	1.37
4	10,923.23	1.60	11,666.61	1.40	12,532.01	1.35
5	11,423.87	1.35	11,788.70	1.50	12,763.42	1.28
Average	11,066.08	1.47	11,848.01	1.37	12,762.93	1.35

TABLE 31

Results for decentralized charging with \$0.25 fixed cost ($n = 100$)

Instance	Penetration rate r					
	20%		35%		50%	
	Energy cost (\$)	PAR	Energy cost (\$)	PAR	Energy cost (\$)	PAR
1	10,719.67	1.31	11,997.42	1.35	12,884.50	1.33
2	10,729.78	1.42	11,860.50	1.43	12,641.90	1.45
3	11,351.14	1.46	11,864.40	1.38	12,728.60	1.28
4	10,936.08	1.48	11,582.04	1.50	12,515.64	1.49
5	11,354.52	1.32	11,724.01	1.42	12,774.66	1.31
Average	11,018.24	1.31	11,805.68	1.42	12,709.06	1.37

TABLE 32

Results for decentralized charging with \$1 fixed cost ($n = 100$)

Instance	Penetration rate r					
	20%		35%		50%	
	Energy cost (\$)	PAR	Energy cost (\$)	PAR	Energy cost (\$)	PAR
1	48,104.46	1.97	50,669.98	1.91	53,642.30	1.87
2	48,119.74	1.98	51,630.14	1.89	53,114.09	1.94
3	48,180.33	1.97	51,508.40	1.90	53,218.79	1.82
4	47,332.32	1.99	51,260.11	1.90	53,801.14	1.88
5	48,503.38	1.97	50,818.31	1.91	54,086.15	1.76
Average	48,048.05	1.97	51,177.39	1.90	53,572.49	1.85

TABLE 33

Results for decentralized charging with \$0 fixed cost ($n = 200$)

Instance	Penetration rate r					
	20%		35%		50%	
	Energy cost (\$)	PAR	Energy cost (\$)	PAR	Energy cost (\$)	PAR
1	43,415.46	1.48	46,524.04	1.40	49,693.17	1.23
2	43,615.71	1.61	46,890.81	1.20	49,426.61	1.30
3	43,482.45	1.40	46,817.15	1.36	49,640.93	1.34
4	43,025.98	1.57	47,158.20	1.42	49,170.51	1.28
5	43,488.48	1.37	46,027.26	1.54	50,344.17	1.28
Average	43,405.62	1.48	46,683.49	1.38	49,655.08	1.29

TABLE 34

Results for decentralized charging with \$0.25 fixed cost ($n = 200$)

Instance	Penetration rate r					
	20%		35%		50%	
	Energy cost (\$)	PAR	Energy cost (\$)	PAR	Energy cost (\$)	PAR
1	43,605.04	1.46	46,153.00	1.55	49,739.43	1.33
2	43,189.48	1.51	47,011.33	1.33	49,834.68	1.31
3	43,637.85	1.48	47,757.72	1.47	49,759.09	1.42
4	42,939.61	1.65	46,924.28	1.40	49,354.90	1.32
5	43,276.01	1.42	45,956.66	1.34	50,484.72	1.30
Average	43,329.60	1.46	46,760.60	1.42	49,834.56	1.34

TABLE 35

Results for decentralized charging with \$1 fixed cost ($n = 200$)

charging scenarios. Figure 4 (a) shows the charging profile when the user is left uncontrolled, which is the same as shown in Figure 2(a). Figure 4(b) depicts user 1’s decentralized charging profile from the DCS with $fc = \$0$. It can be observed that user 1 charges the vehicle from 8am ($t = 17$) to 9am ($t = 19$), from 10am ($t = 21$) to 11am ($t = 23$) and from 1pm ($t = 27$) to 1:30pm ($t = 28$). The day-time charging of 5 half-hour intervals is divided into three sections. The allocation of these charging periods is given by the heuristic algorithm in minimizing user1’s energy cost based on the price at the specific time. Figures 4(c) and 4(d) show the decentralized charging profile for user 1 from the DCS with $fc = \$0.25$ and $fc = \$1$, respectively. When $fc = \$0.25$, user 1 charges the vehicle from 1:30pm ($t = 28$) to 4pm ($t = 33$), and his/her entire day-time charging of 5 half-hour intervals is assigned in to the only one section. The latter is a direct result of the fixed cost of $\$0.25$. Similarly, when $fc = \$1$, this charging profile has a total of 2.5 consecutive charging hours (or 5 consecutive half hour intervals) during the day between 8am ($t = 17$) to 10:30am ($t = 22$), thus drawing a total of 8.25 kWh of energy. Nonetheless, the charging schedule during the evening hours is not subject to the fixed setup cost. Therefore, for example in Figure 4(d), user 1 is scheduled to charge for only one interval at 1:30am ($t = 4$), and to charge for five consecutive intervals from 3:30am ($t = 8$) to 6am ($t = 13$).

Tables 36 and 37 compare the energy cost and PAR for decentralized and centralized charging solutions under different fc . Again, for each combination of (n, r) , the energy cost and the gap reported in the table are the averages over 5 instances. The gap in these two tables measures the effectiveness of the decentralized charging scheduling, referred to as “DCS”, when compared to the OCS solution. The lower the gap is, the closer the DCS solution is to the OCS solution, and the more effective the DCS solution is. The gap on energy cost is calculated as $\frac{\text{energy cost of (DCS)} - \text{energy cost of (OCS)}}{\text{energy cost of (OCS)}}$ and the gap on PAR is calculated as $\frac{\text{PAR of (DCS)} - \text{PAR of (OCS)}}{\text{PAR of (OCS)}}$. From Tables 36 and 37, the average gaps on energy cost for $fc = \$0.25$ and $fc = 1$ are approximately 1.8% and 2.4%, respectively. However, for $fc=0$, the average gap is about 10%, which might still be acceptable given the

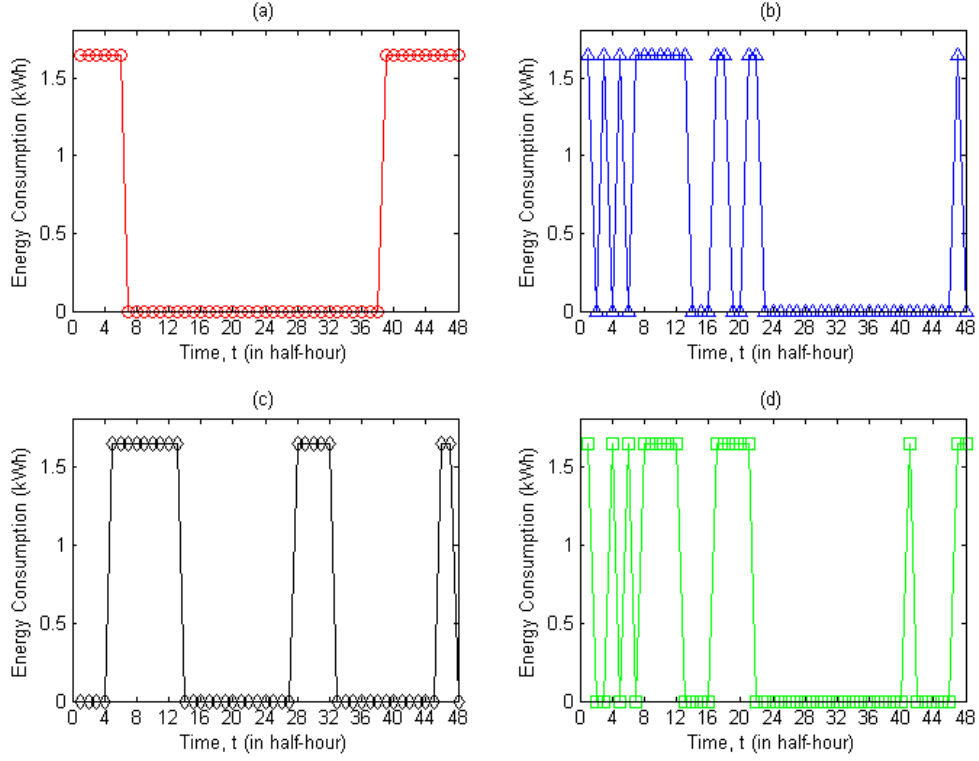


Figure 4. Four scenarios of charging profile for user 1 under uncontrolled and DCS model

fc (\$)	n	r	10			50		
			20%	35%	50%	20%	35%	50%
0	Energy cost (\$)	OCS	143.50	148.67	159.52	2,771.95	3,011.39	3,214.50
		DCS	158.21	159.63	172.76	3,123.17	3,328.92	3,050.27
		Gap	10.25%	7.37%	8.30%	12.67%	10.54%	9.05%
	PAR	OCS	1.15	1.16	1.13	1.09	1.06	1.05
		DCS	1.98	1.91	1.88	1.98	1.92	1.87
		Gap	72.17%	64.66%	66.37%	81.65%	81.13%	78.10%
0.25	Energy cost (\$)	OCS	143.69	148.89	159.67	2,782.88	3,015.56	3,215.34
		DCS	144.73	150.46	164.18	2,829.03	3,067.12	3,285.86
		Gap	0.72%	1.06%	2.82%	1.66%	1.71%	2.19%
	PAR	OCS	1.13	1.17	1.15	1.09	1.10	1.07
		DCS	1.30	1.37	1.55	1.43	1.37	1.34
		Gap	15.04%	17.09%	34.78%	31.19%	24.55%	25.23%
1	Energy cost (\$)	OCS	144.51	149.40	159.71	2,774.71	3,014.67	3,217.34
		DCS	146.95	159.50	168.60	2,813.92	3,045.35	3,274.03
		Gap	1.69%	6.77%	5.57%	1.41%	1.02%	1.76%
	PAR	OCS	1.18	1.17	1.13	1.10	1.07	1.08
		DCS	1.54	1.95	1.85	1.39	1.32	1.43
		Gap	30.51%	66.67%	63.72%	26.36%	23.36%	32.41%

TABLE 36

Comparisons between the (OCS) and (DCS) models under three fixed cost ($n=10$ and $n=50$) scenarios

fc (\$)	n r	100			200			
		20%	35%	50%	20%	35%	50%	
0	Energy cost (\$)	OCS	10,822.68	11,623.08	12,527.74	42,476.37	45,831.21	48,886.61
		DCS	12,215.81	12,876.96	13,713.10	48,048.05	51,177.39	53,572.49
		Gap	12.87%	10.79%	9.46%	13.12%	11.66%	9.59%
	PAR	OCS	1.07	1.04	1.04	1.08	1.04	1.03
		DCS	1.98	1.98	1.84	1.98	1.90	1.85
		Gap	85.05%	90.38%	76.92%	83.33%	82.69%	79.61%
0.25	Energy cost (\$)	OCS	10,823.87	11,623.45	12,528.37	42,477.86	45,832.94	48,888.29
		DCS	11,066.08	11,848.01	12,762.93	43,405.62	46,683.49	49,655.08
		Gap	2.24%	1.93%	1.87%	2.18%	1.86%	1.57%
	PAR	OCS	1.07	1.04	1.04	1.08	1.04	1.03
		DCS	1.41	1.37	1.35	1.48	1.38	1.29
		Gap	31.78%	31.73%	29.81%	37.04%	32.69%	25.24%
1	Energy cost (\$)	OCS	10,825.91	11,628.42	12,537.04	42,482.11	45,838.41	48,898.27
		DCS	11,018.24	11,805.68	12,709.06	43,329.60	46,760.60	49,834.56
		Gap	1.78%	1.52%	1.37%	1.99%	2.01%	1.91%
	PAR	OCS	1.07	1.06	1.09	1.08	1.04	1.05
		DCS	1.40	1.42	1.37	1.50	1.42	1.34
		Gap	30.84%	33.96%	25.69%	38.89%	36.54%	27.62%

TABLE 37

Comparisons between the (OCS) and (DCS) models under three fixed cost ($n=100$ and $n=200$) scenarios

benefit of not having a central controller. For the peak-to-average ratio, there is a much larger gap between the DCS and OCS solutions for all combinations of n , r and fc . In particular, for $fc = \$0$, $\$0.25$ and $\$1$, the average gaps on PAR are approximately 78.5%, 28% and 36%, respectively.

Finally, Figure 5 illustrates a comparison of load leveling achieved through three charging scenarios, i.e. uncontrolled charging scenario (the ‘o’ series), the OCS solution with $\$0.25$ fixed cost (the ‘ Δ ’ series), and the DCS solution with $\$0.25$ fixed cost (the ‘ \diamond ’ series) in a case of $n = 10$ users. It can be observed that the OCS solution presents the best load leveling, and the DCS solution has a few modest peaks and valleys. This is consistent with the observation that the gap on PAR is relatively high as illustrated in Tables 36 and 37. However, the DCS solution still provides significantly better scheduling compared to the uncontrolled solution which has large peaks and valleys. While it may not be as effective as the centralized solution in minimizing the energy cost and leveling the load, the decentralized solution can be appealing because users decide their own charging scheduling.

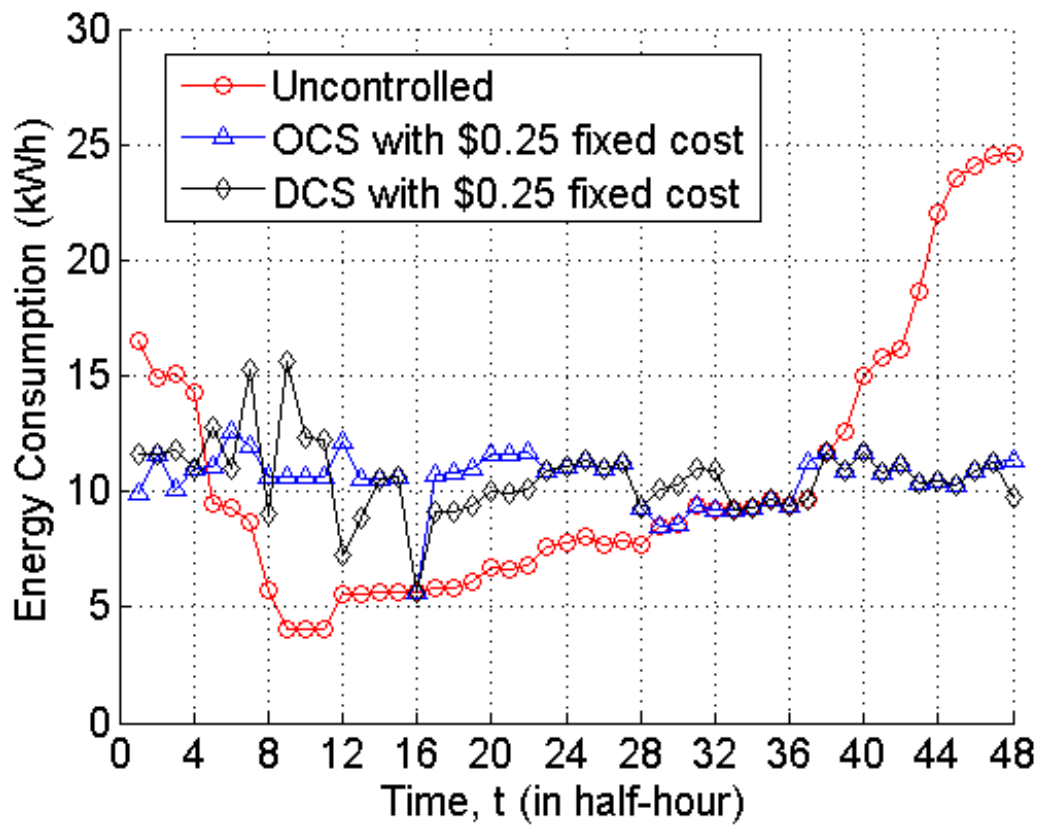


Figure 5. Comparison of load leveling under different models ($n=10$)

CHAPTER 5

CONCLUSION AND FUTURE WORK

5.1 Conclusions

In order to mitigate the adverse effect of extra loads due to EV charging on the existing power grid, this thesis studies the optimal charging scheduling problem that coordinates the charging of all EV users in a power distribution network. The contribution of the thesis is three-fold. First, setup cost at commercial charging stations during day-time is explicitly modeled in order to reduce the frequency of switch on/off a charger. Second, users' daily commute schedule is considered in the model to determine the subsequent charging pattern. Third, battery capacity is considered in the proposed charging scheduling.

Particularly, we employ the mixed integer program model to optimize the EV charging schedule. The objective is to minimize the sum of: 1) for all users while meeting each user's household and EV charging demands, energy cost and 2) the total setup costs. Considerations are given to the "state of charge" for EVs, fixed setup cost, charging patterns and battery capacity.

Numerical results show that the OCS model significantly reduces the energy cost and the PAR, when compared to uncontrolled charging scheduling. In most cases, the energy cost for the OCS solution is 18% lower than that of the uncontrolled charging solution, and the PAR value is at least 50% lower. In addition, including fixed setup costs in the OCS model drastically reduces the percentage of non-consecutive charging (by approximately 80% for $fc = \$0.25$ or $fc = \$1$, when compared to $fc = \$0$) without notable losses in total energy cost, the

PAR and load leveling. This is very encouraging from the perspective of grid stability. Furthermore, a rolling horizon heuristic algorithm is proposed for solving large-scale OCS problems efficiently. Numerical results reveal an average gap of approximate 5% between the energy costs of the heuristic and OCS solutions.

In addition, a decentralized coordinate search heuristic is developed for EV users to determine their own charging schedules in a distributed manner. Numerical results show that while the centralized solution is most effective in reducing both energy cost and peak-to-average ratio, and the proposed decentralized solution is competitive in reducing energy cost, with less than 2% optimality gap in most cases. Although on average 30% less effective than the OCS solution, the DCS solution still achieves far better load leveling when compared to the uncontrolled charging. The improvement over the uncontrolled charging is approximately 15% on total energy cost and 30% on PAR. Nonetheless, DCS is still considered highly appealing to utility companies because its distributed nature.

5.2 Future Work

There are several future research directions. First, several meta-heuristics will be studied to improve the solutions by the rolling horizon heuristic for the centralized charging scheduling problem. Second, the centralized optimization model in this thesis is essentially mixed integer programs, which cannot be solved efficiently by general purpose solvers for large-scale instances. Thus, developing customised solution methods such as Lagrangian relaxation is another interesting problem. Third, we would like to develop a decentralized solution that accounts for demand stochasticity using agent-based simulation. Finally, we would like to integrate control-based constraints in the charging scheduling models so that the grid stability is guaranteed.

REFERENCES

- [1] The Energy Foundation. (2010). *The Energy Foundation 2010 Annual Report*. Retrieved December 19, 2012, from http://www.ef.org/documents/2010_Annual_Report.pdf.
- [2] Pavley Car Standards. *Assembly Bill No. 1493*. Retrieved November 15, 2012, from <http://www.arb.ca.gov/cc/ccms/documents/ab1493.pdf>.
- [3] Becker, T. (2009). *Electric Vehicles in the United States A New Model with Forecasts to 2030*. Retrieved December 14, 2012, from <http://www.reffcon.com/media/downloads/8.pdf>
- [4] Rahman, S. and Shrestha, G.B. (1993). An investigation into the impact of electric vehicle load on the electric utility distribution system. *IEEE Transactions on Power Delivery*. 8(2), 591-597.
- [5] Ranmanathan, B. and Vittal, V. (2008). A framework for evaluation of advanced direct load control with minimum disruption. *IEEE Transactions of Power Systems*. 23(4), 1681-1688.
- [6] Pedrasa, M., Spooner, T., and MaxGill, I. (2009). Scheduling of demand side resources using binary particle swarm optimization. *IEEE Transactions on Power Delivery*. 24(3), 1173-1181.
- [7] Collins, M. and Mader, G. (1983). The timing of EV recharging and its effect on utilities. *IEEE Transactions on Vehicular Technology*. 32(1), 90-97.
- [8] Koyanagi, F. and Uriu, Y. (1998). A strategy of load leveling by charging and discharging time control of electric vehicles. *IEEE Transactions on Power Systems*. 13(3), 1179-1184.

- [9] Alternative Fuels and Advanced Vehicles Data Center of U.S. Department of Energy, *All-electric vehicle basics*. Retrieved August 26, 2012, from http://www.afdc.energy.gov/vehicles/electric_basics_ev.html.
- [10] Rosen, J.B. (1965). Existence and Uniqueness of Equilibrium Points for Concave N -person Games. *Econometrica*. 33(3), 520–534.
- [11] Agnetis, A., De Pascale, G. and Pranzo, M. (2009). Computing the Nash solution for scheduling bargaining problems. *International Journal of Operational Research*. 6(1), 54-69.
- [12] Balijepalli, V.S.K.M., Pradhan, V. and Khaparde, S.A. 2011, ‘Review of Demand Response under Smart Grid Paradigm’, *Innovative Smart Grid Technologies-India (ISGT India), 2011 IEEE PES*. 236-243.
- [13] Bonneville, E. and Rialhe, A. (2006). Demand Side Management for residential and commercial end-users. *Efficiency & eco-design*. 2006(May), 1-11.
- [14] Zhang, D., Papageorgiou, L.G., Samsatli, N.J. and Shah, N. (2011, May 22-27). Optimal scheduling of smart homes energy consumption with microgrid. *The First International Conference on Smart Grids, Green Communications and IT Energy-aware Technologies*. Venice, Italy, 70-75.
- [15] Vandael, S., Boucke, N., Holvoet, T., and Deconinck, G. (2010, May 10-14). Decentralized demand side management of plug-in hybrid vehicles in a smart grid. *Proceedings of First International Workshop on Agent Technologies for Energy Systems (ATES 2010)*. Toronto, Canada, 67-74.
- [16] Ramchurn, S., Vytelingum, P., Rogers, A. and Jennings, N. (2011, May 2-6). Agent-based control for decentralized demand side management in the smart grid. *The Tenth International Conference on Autonomous Agents and Multiagent Systems (AAMAS 2011)*. Taipei, Taiwan, 5-12.
- [17] Kowahl, N. and Kuh, A. (2010, July 18-23). Micro-scale smart grid

- optimization. *The 2010 International Joint Conference on Neural Networks (IJCNN)*. Barcelona, Spain, 1-8.
- [18] Clement-Nyns, K., Haesen, E. and Driesen, J. (2010). The impact of charging plug-in hybrid electric vehicles on a residential distribution grid. *IEEE Transactions on Power Systems*. 25(1), 371-380.
- [19] Mohsenian-Rad, A.H., Wong, V.W.S., Jatskevich, J. and Schober, R. (2010, January 19-21). Optimal and autonomous incentive-based energy consumption scheduling algorithm for smart grid. *2010 Innovative Smart Grid Technologies (ISGT)*. Gaithersburg, MD, 1-6.
- [20] Vytelingum, P., Voice, T.D., Ramchurn, S.D., Rogers, A. and Jennings, N.R. (2010, May 10-14). Agent-based micro-storage management for the smart grid. *The Ninth International Conference on Autonomous Agents and Multiagent Systems (AAMAS 2010)*, Toronto, Canada, 39-46.
- [21] Fan, Z. (2010). Distributed demand response and user adaptation in smart grids. *arXiv:1007.5425 [cs.NI]*. 1-6.
- [22] Clement, K., Haesen, E. and Driesen, J. (2009, March 15-18). Coordinated charging of multiple plug-in hybrid electric vehicles in residential distribution grids. *Power Systems Conference and Exposition (PSCE '09)*, Seattle, WA, 1-6.
- [23] Mets, K., Verschueren, T., Haerick, W., Develder, C. and Turck, F.D. (2010, April 19-23). Optimizing smart energy control strategies for plug-in hybrid electric vehicle charging. *2010 IEEE/IFIP Network Operations and Management Symposium Workshops (NOMS Wksps)*. Osaka, Japan, 293-299.
- [24] Sundström, O. and Binding, C. (2010). *Optimization Methods to Plan the Charging of Electric Vehicle Fleets*. Retrieved February 20, 2013, from http://www.zurich.ibm.com/pdf/csc/EDISON_ccpe_main.pdf.
- [25] Xu, Y. and Pan, F. (2012, December 10-13). Scheduling for Charging Plug-in

- Hybrid Electric Vehicles. *51st IEEE Conference on Decision and Control*. Maui, HI, 2495-2501.
- [26] Rautiainen, A., Repo, S., Järventausta, P., Mutanen, A., Vuorilehto, K. and Jalkanen, K. (2012). Statistical charging load modeling of PHEVs in electricity distribution networks using national travel survey data. *IEEE Transactions on Smart Grid*. 3(4), 1650-1659.
- [27] Mohsenian-Rad, A.H. and Leon-Garcia, A. (2010). Optimal residential load control with price prediction in real-time electricity pricing environments. *IEEE Transactions on Smart Grid*. 1(2), 120-133.
- [28] Samadi, P., Mohsenian-Rad, A.H., Schober, R., Wong, V.W.S. and Jatskevich, J. (2010, October 4-6). Optimal Real-time Pricing Algorithm Based on Utility Maximization for Smart Grid. *2010 First IEEE International Conference on Smart Grid Communication (SmartGridComm)*. Gaithersburg, MD, 415-420.
- [29] Bonabeau, E. (2002). Agent-based modeling: Methods and techniques for simulating human systems. *Proceedings of the National Academy of Science*. 99(3), 7280-7287.
- [30] Ma, Z., Callaway, D. and Hiskens, I. (2013). Decentralized charging control for large populations of plug-in electric vehicles. *IEEE Transactions on Control Systems Technology*. 21(1), 67-78.
- [31] Phan, D.T., Xiong, J. and Ghosh, S. (2012, June 27-19). A Distributed Scheme for Fair EV Charging Under Transmission Constraints. *2012 American Control Conference*. Montréal, Canada, 1053-1058.
- [32] Shahidehpour, M., Yamin, H. and Li, Z. (2002). *Market operations in electric power systems: forecasting, scheduling and risk management*. New York: John Wiley and Sons Inc.
- [33] Aigner, D. (1985). The residential electricity time-of-use pricing experiments:

- what have we learned?. In Hausman, J.A. and Wise, D.A. (Eds.). *Social Experimentation*, Chicago: University of Chicago Press, 11-53.
- [34] Baladi, S.M., Herriges, J.A. and Sweeney, J.T. (1998). Residential response to voluntary time-of-use electricity rates. *Resource and Energy Economics*. 20(1998), 225-244.
- [35] Davis, M.B. and Bradley, T.H. (2012). The efficacy of electric vehicle time-of-use rates in guiding plug-in hybrid electric vehicle charging behavior. *IEEE Transactions on Smart Grid*. 3(4), 1679-1686.
- [36] Hartway, R., Price, S. and Woo, C.K. (1999). Smart meter, customer choice and profitable time-of-use rate option. *Energy*. 24(10), 859-903.
- [37] Fetz, A. and Filippini, M. (2010). Economies of vertical integration in the Swiss electricity sector. *Energy Economics*. 32(6), 1325-1330.
- [38] Martínez-Budría, E., Jara-Díaz, S. and Ramos-Real, F.J. (2003). Adapting productivity theory to the quadratic cost function: an application to the Spanish electric sector. *Journal of Productivity Analysis*. 20(2), 213-229.
- [39] Nissan USA. *Nissan LEAF: features and specifications*. Retrieved November 1, 2012, from <http://www.nissanusa.com/leaf-electric-car/specs-features/index#/leaf-electric-car/>.
- [40] Ipakchi, A. and Albuyeh, F. (2009). Grid of the future. *IEEE Power and Energy Magazine*. 7(2), 52-62.
- [41] Southern California Edison. *Residential rates*. Retrieved November 4, 2012, from <http://www.sce.com/residential/rates/special-time-of-use.htm>.
- [42] NAHB Research Center Inc. (2001). *Review of residential electrical energy use data*. Retrieved August 15, 2012, from <http://www.toolbase.org/PDF/CaseStudies/ResElectricalEnergyUseData.pdf>.

CURRICULUM VITAE

NAME: Guangyang Xu

ADDRESS: Department of Industrial Engineering
University of Louisville
Louisville, KY 40292

EDUCATION: B.S. Chemical Engineering
China University of Mining and Technology (Beijing)
2004

**PREVIOUS
RESEARCH:** Logistics
Operations Research
Optimization

AWARDS: Leigh Ann Conn Graduate Fellowship - 2012
Industrial Engineering Graduate Student Award - 2013
Alpha Pi Mu (Industrial Engineering Honor Society)